UNIVERSITY OF KWAZULU-NATAL

Link Adaptation for Quadrature Spatial Modulation

Segun Emmanuel Oladoyinbo

2016

Link Adaptation for Quadrature Spatial Modulation

By Segun Emmanuel Oladoyinbo

Student Number: 214574841

Submitted in fulfilment of the academic requirements of

Master of Science in Engineering

School of Engineering

College of Agriculture, Engineering and Science

University of KwaZulu-Natal

Howard College

South Africa

Supervised by: Dr Narushan Pillay

Co-supervised by: Prof HongJun Xu

July 2016

CERTIFICATION

As the candidate's Supervisor I agree to the submission of this dissertation.

_____

Signed: Dr Narushan Pillay

Date: 28th July, 2016

DECLARATION 1 - PLAGIARISM

I, Segun Emmanuel Oladoyinbo declare that:

1. The research reported in this dissertation, except where otherwise indicated, is my original research.
2. This dissertation has not been submitted for any degree or examination at any other university.
3. This dissertation does not contain other persons' data, pictures, graphs or other information, unless specifically acknowledged as being sourced from other persons.
4. This dissertation does not contain other persons' writing, unless specifically acknowledged as being sourced from other researchers. Where other written sources have been quoted, then:

a. Their words have been re-written but the general information attributed to them has been referenced

b. Where their exact words have been used, then their writing has been placed in italics and inside quotation marks, and referenced.

5. This dissertation does not contain texts, graphics or tables copied and pasted from the internet, unless specifically acknowledged, and the source being detailed in the thesis and in the Reference section.

_____

Signed: Oladoyinbo Segun

Date: 28th July, 2016

DECLARATION 2 - PUBLICATIONS

The work in this dissertation will be submitted to IET communications journal for publication. The detail is as follows:

S. Oladoyinbo, N. Pillay, H. Xu "Adaptive quadrature spatial modulation," [*Ready for submission to IET Communications Journal*].

_____

Signed: Oladoyinbo Segun

Date: 28th July, 2016

ACKNOWLEDGEMENTS

I want to give all the glory to God for the gift of life and the strength granted onto me in the course of this research and for making it a possibility "…but with God all things are possible, **Matthew 19:26** ".

My gratitude goes to my supervisors, Dr Narushan Pillay and Prof H. Xu, for your time, encouragement, training as a researcher from wealth of experience, guidance and unlimited access to your office anytime I come around for help during this period. To my family members, I say a big thank you. My parents: Elder. P.O Oladoyinbo and Mrs W.A Oladoyinbo deserve a bigger thank you for their encouragement, may you live long to enjoy the fruit of your labour in Jesus name. Desire (Ajike mi), Ayobami, Ife, Olayide (Aduke temi ni kan), Ashaolus' and Seun Oyebode are not left out. Finally, to my loved ones, brothers, friends and well-wishers, thank you all for your supports, motivations and prayers. Gracias

DEDICATION

This dissertation is dedicated to my lovely wife, Olayide Adebimpe and my beautiful daughter Desire Lois.

ABSTRACT

Quadrature spatial modulation (QSM) maintains all of the advantages of spatial modulation but further improves upon its spectral efficiency by the logarithm base two of the number of transmit antennas. However, further improvement in terms of reliability can still be achieved. On this note, in this dissertation, link adaptation for QSM is investigated.

The existing analytical error performance for QSM does not agree well with Monte Carlo simulation results in the low signal-to-noise ratio (SNR) region. Therefore, the first contribution is a lower bound approach to the analytical error performance, which agrees well with simulation results for low to high SNRs.

Secondly, link adaptation is investigated on conventional QSM system to further improve upon the reliability of the system (QSM). Assuming a slowly varying channel and full knowledge thereof, the proposed scheme is based on employing unique candidate transmission modes, chosen to satisfy a target spectral efficiency. The proposed scheme employs optimal transmit antenna selection and constellation selection so as to minimize the instantaneous bit error probability (IBEP). The candidate mode with the minimum IBEP is activated for transmission. Significant SNR gain is demonstrated by the proposed scheme over QSM.

Finally, the effects of low-complexity transmit antenna selection for AQSM scheme is investigated to further reduce the computational complexity (CC) overhead. The selection is based on computing the channel amplitude and antenna correlation to eliminate the poor channel(s). Monte Carlo simulation results demonstrate a trade-off between CC and reliability in comparison to the use of optimal antenna selection.

TABLE OF CONTENTS

LIST OF FIGURES

LIST OF TABLES

LIST OF ACRONYMS

APM……..Amplitude/Phase Modulation
AQSM……Adaptive Quadrature Spatial Modulation
AQSM-EDAS……Adaptive Quadrature Spatial Modulation based on EDAS
AQSM-LCTAS……Adaptive Quadrature Spatial Modulation based on LCTAS
ASM……..Adaptive Spatial Modulation
AWGN ……..Additive White Gaussian Noise
BER……Bit Error Rate
BPSK…….Binary Phase Shift Keying
CC…….Computational Complexity
CSI…….Channel State Information
EDAS……..Euclidean Distance Antenna Selection
FRFC……...Frequency-Flat Rayleigh Fading channel
GSM……..Generalized Spatial Modulation
i.i.d. …….Independent and Identically Distributed
IAS……..Inter-Antenna Synchronization
IBEP……Instantaneous Bit Error Probability
ICI……..Inter-Channel Interference
IEEE……..Institute of Electrical and Electronic Engineers
ISI……Inter-Symbol Interference
LCTAS……Low-Complexity Transmit Antenna Selection
LCTAS-A-C……LCTAS based on Channel Amplitude and Antenna Correlation

MA-GSM……Multiple Active Transmit Antenna for Generalized Spatial Modulation
MGF……..Moment Generating Function
MIMO……Multiple-Input Multiple-Output
ML…….Maximum Likelihood
PDF……Probability Density Function
PEP…….Pairwise Error Probability
PSK……Phase Shift Keying
QAM……Quadrature Amplitude Modulation
QPSK…….Quadrature Phase Shift Keying
QSM……Quadrature Spatial Modulation
RF……..Radio Frequency
SER……Symbol Error Rate
SM……..Spatial Modulation

SM-OD……Spatial Modulation with Optimal Detection

SMUX……..Spatial Multiplexing

SNR……...Signal-to-Noise Ratio

STBC…….Space-Time Block Code

SVD…….Signal Vector Based Detection

TAS……..Transmit Antenna Selection

V-BLAST……Vertical Bell Laboratories Layered Space-Time Architecture

CHAPTER 1

INTRODUCTION

1 Multiple-Input Multiple-Output

Multiple-input multiple-output (MIMO) systems have shown tremendous promise over the years with regards to its high transmission capacity and superior system reliability in a wireless communication scenario [1]. Traditionally, the data to be transmitted in MIMO systems is encoded and divided into parallel data streams, each of which is modulated by a separate transmitter. During transmission, the data streams are captured by multiple antennas, which are slightly different in phase, each antenna can be treated as a separate channel in MIMO systems. The antenna takes advantage of the multiple channels to transfer data, thus, increasing throughput [2]. The data rate per channel increases linearly with the number of different data streams that are transmitted in the same channel, providing scalability and a more reliable link.

MIMO systems have the benefit of increase in capacity, transmission range and robustness, such that it permits multiple data streams. In addition, it helps to improve the signal-to-noise ratio (SNR) and reliability significantly. However, due to the simultaneous transmission of data in MIMO systems, inter-antenna synchronization (IAS) is required at the transmitter and inter-channel interference (ICI) is experienced at the receiver [1, 3].

1.1 Categories and Techniques of MIMO

In [4], MIMO systems are categorized according to their transmission techniques, which can be divided into three main categories. These are as follows:

1. Spatial multiplexing: Signals are split into bit streams and each stream is transmitted from a different transmit antenna in the same frequency channel. If the signals arrive at the receiver with highly different spatial signatures and accurate channel state information (CSI), the receiver can separate the bit stream into a perfect parallel channel. The maximum number of streams that the signal can be split into is limited by the number of available transmit antennas [1, 3]. Similarly, the assumption of known CSI in spatial multiplexing can be used with precoding [5]. Spatial multiplexing can be employed for simultaneous transmission to multiple receivers (space division multiple access) [6], which requires the knowledge of the CSI at the transmitter as good separability is achieved with scheduling receivers.

2. Diversity coding: The term ‘diversity’ has been given different meanings over time in wireless communication scenarios. The variation of the channel in time, frequency and space with multiple copies of data arriving at the receiver can be defined as diversity. The amount of improvement that can be achieved in terms of the received signal (in diversity scheme) depends on the fading characteristics of the transmitted signal. This technique exploits the independent fading in the channel to enhance the reliability of the system. In diversity coding, the knowledge of the CSI is not needed at the transmitter as a single stream of data is transmitted; but the transmitted signal is coded with a technique called space-time coding prior to transmission [4].
3. Precoding: This is a type of transmit diversity technique which sends out pre-coded information to the receiver according to the known CSI, employing multi-stream beamforming. The signal is transmitted from each of the available transmit antennas with the appropriate phase and amplitude in order to maximize the SNR and transmitting power. Precoding techniques have the benefit of summing up the transmitted signals from different antennas, constructively at the receiver. Thus, increasing the signal gain at the receiver and reducing fading effects. However, knowledge of the CSI is required at the transmitter for precoding, to assist in maximizing the signal level at the receiver [4].

1.2 System Model for a MIMO System

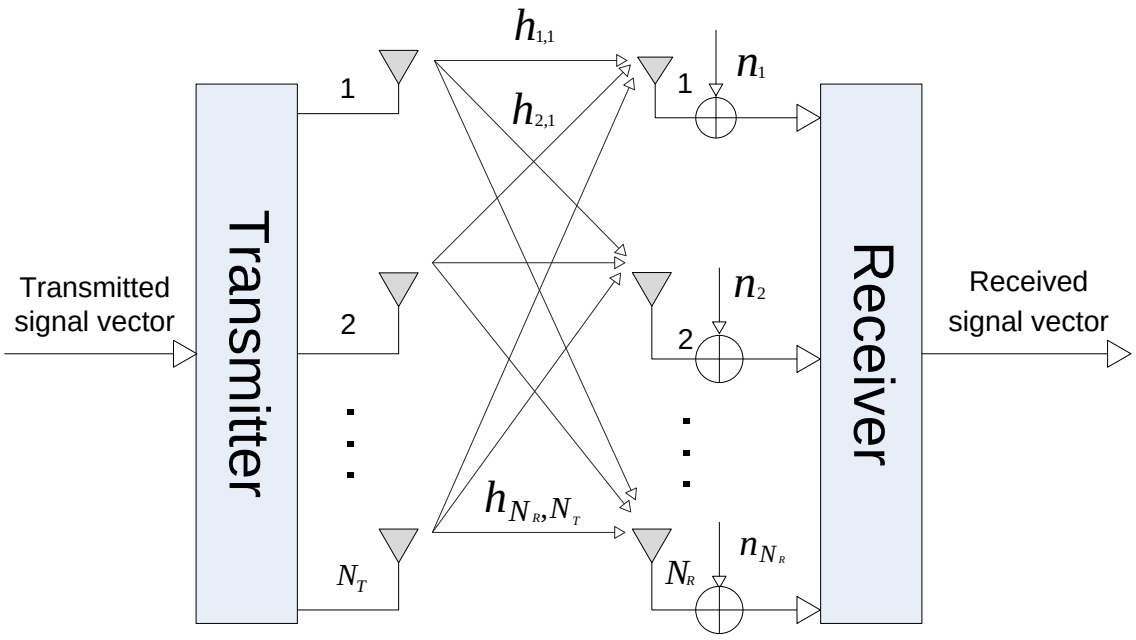

Figure 1-1 System Model for a MIMO system [7]

Figure 1-1 illustrates a typical MIMO system with N_T transmit antennas and N_R receive antennas with multipath fading channel $\boldsymbol{H}$ between the transmitter and the receiver. The respective path of the channel $\boldsymbol{H}$ used for transmission with a constant channel gain can be represented as:

$$\boldsymbol{H} = [\boldsymbol{h}_1 \ \boldsymbol{h}_2 \ \boldsymbol{h}_3 \ \dots \ \boldsymbol{h}_{N_T}]^T \tag{1-1}$$

The channel matrix between the transmit antennas N_T and receive antennas N_R with dimension $N_R \times N_T$ can be expressed as:

$$\boldsymbol{H} = \begin{bmatrix} h_{1,1} & \cdots & h_{1,N_T} \\ \vdots & \ddots & \vdots \\ h_{N_R,1} & \cdots & h_{N_R,N_T} \end{bmatrix} \tag{1-2}$$

where $h_{i,j}$ is the corresponding row and column of the channel $\boldsymbol{H}$, respectively, used for transmission at a particular time t, i. e. $i \in [1: N_R]$ and $j \in [1: N_T]$.

Wireless channels are categorized into large-scale fading and small-scale fading [8].

1. Large-scale fading is distance dependant, as signal power decreases over time due to path loss of the transmitted signal and foliage in the signal path.
2. Small-scale fading occurs due to multipath of the channel resulting to the distortion of the signal in amplitude, phase and angle of arrival. It is caused by multipath of the signal propagation.

In this dissertation, a frequency-flat Rayleigh fading channel is used. This is mostly seen in an environment with high environmental propagation effect on the radio wave or where line of sight (LOS) is absent. Especially, in the urban areas where there are large number of reflectors.

A signal $\boldsymbol{x}$ of dimension $N_T \times 1$, i.e. $\boldsymbol{x} = [x_1 \ x_2 \ x_3 \dots x_{N_T}]^T$ is transmitted over the MIMO multipath fading channel $\boldsymbol{H}$ as shown in the Figure 1-1. This is considered in the presence of additive white Gaussian noise (AWGN) represented by a vector $\boldsymbol{n}$ of dimension $N_R \times 1$, i.e.

$\boldsymbol{n} = \left[n_1 \;\; n_2 \;\; n_3 \ldots \; n_{N_R}\right]^T$ with Gaussian distribution $CN\,(0,1)$ and with independent and identically distributed (i.i.d) entries. Then, the received signal $\boldsymbol{y}$ becomes:

$$\boldsymbol{y} = \sqrt{\rho}\,\boldsymbol{H}\boldsymbol{x} + \boldsymbol{n} \tag{1-3}$$

where ρ is the average SNR.

Note, the channel used is a frequency-flat Rayleigh multipath fading channel between the transmitter and the receiver, such that the bandwidth of the signal $\boldsymbol{x}$ is less than the coherence bandwidth of the channel $\boldsymbol{H}$ resulting in a constant channel gain over the transmitted signal bandwidth.

Despite the advantages of MIMO systems, it still has some limitations such as the need for IAS at the transmitter due to the simultaneous transmission of data, high power consumption considering all the antennas are active at the same time and ICI is experienced at the receiver considering all transmit antennas are transmitting at the same time.

In the next sub-section, techniques used to improve the limitations of conventional MIMO systems will be discussed and examples of MIMO systems including innovative forms of MIMO will be presented in Section 1.3.

1.3 Innovative Forms of MIMO

Spatial multiplexing is a suitable scheme for future wireless communication due to the high demand for capacity in multimedia services. However, coupling of symbols in time and space in spatial multiplexing causes high ICI and simultaneous transmission of data requires IAS at the transmitter [8]. These are the major limitations of spatial multiplexing. The reliability of the MIMO system is key, in which spatial diversity plays a major role. However, spatial diversity techniques have a major limitation of ISI due to the dispersion of the channel. This can be avoided if enough space is left between the transmitted symbols. Although, this will cause decreased throughput [9, 10]. Various examples of innovative systems, employing spatial multiplexing and spatial diversity will be discussed in the next sub-section, starting with a prominent example of MIMO system, the Vertical-Bell Laboratories Layered Space-Time Architecture (V-BLAST) [11].

1.3.1 Vertical-Bell Laboratories Layered Space-Time Architecture

V-BLAST employs spatial multiplexing to increase the spectral efficiency of the system by sending out N_T (total number of the available transmit antennas) signals at each time slot. This results to increase throughput by dividing the input bit stream into sub-streams and transmitting it in parallel through a specific antenna. However, ICI and IAS exists in V-BLAST technology, since all transmit antennas transmit data streams simultaneously [11].

In an indoor environment a spectral efficiency of 20 b/s/Hz can be achieved in V-BLAST technology assuming a practical SNR range [11]. In addition, a block of N_T symbols is compressed into a single symbol prior to transmission, so that an algorithm that maps the symbol to just one of the N_T can be employed to retain the information, ICI experienced at the receiver can be avoided [12].

1.3.2 The Alamouti Space-Time Block Code

The Alamouti Space-Time Block Code (STBC) [13], is an example of an improved MIMO system. The Alamouti STBC exploits spatial diversity to improve the reliability of the system by sending two symbols in its first time slot such as x_1 and x_2. The negative conjugate of the second symbol sent in the first time slot, i.e. $(-x_2^*)$ together with the conjugate of the first symbol, i.e. (x_1^*) is sent during the second time slot such that, the transmitted signal $\boldsymbol{X} = \begin{bmatrix} x_1 & x_2 \\ -x_2^* & x_1^* \end{bmatrix}$.

Since, this still requires two time slots to send out two symbols, the data rate remains the same [13, 14]. But, the reliability of the link has improved due to the redundant copies of data transmitted to the receiver over an independent channel. However, in the Alamouti STBC, the computational complexity (CC) at the receiver increases exponentially with the size of the constellation, which makes the implementation not only difficult but expensive [13].

1.3.3 Spatial Modulation

Spatial Modulation (SM) [15-17], is another innovative form of MIMO system proposed by Mesleh *et al.*. SM eliminates the major limitations of IAS and ICI experienced in conventional MIMO by employing multiple transmit antennas in an innovative manner. This is made possible by using a dimension called the spatial (antenna) dimension to convey additional information. In SM, only one transmit antenna is active at each transmission instant, eliminating the need for IAS at the transmitter and ICI at the receiver. Additionally, SM uses the space modulation technique to enhance the error performance and capacity of the system [16]. The Monte Carlo

simulation results for SM demonstrates significant improvement in terms of error performance over V-BLAST [15].

1.3.3.1 Features of Spatial Modulation

The main features of SM are listed below:

1. Single RF chain is used to make the system more cost effective and energy efficient [16].
2. ICI and IAS are totally avoided in SM [16].
3. High spectral efficiency is achieved in SM [15, 16].

The benefits of SM, which includes: reduction in hardware cost, high energy efficiency, elimination of major limitations experienced in conventional MIMO system and increase in throughput with improved error performance, makes SM one of the most promising MIMO systems.

Despite the advantages, SM still has few limitations such as:

1. It requires transmit antennas in the power of two.
2. Its data rate enhancement increases only in logarithm base-two of the total number of transmit antennas compared to other spatial multiplexing techniques.
3. Transmit diversity was not exploited in SM

Due to clear advantages of SM, we present a detailed survey of the primary works of SM. In the next sub-section, improvement achieved in SM in terms of error performance, CC and spectral efficiency will be discussed.

1.3.3.2 Improvement Achieved in SM in Terms of Error Performance and CC

Application of transmit diversity and receive diversity or a combination of both in MIMO systems allow huge improvement to be achieved in terms of error performance [18]. Furthermore, introducing transmit antenna selection (TAS) into a system can further improve its error performance [18].

1.3.3.3 Transmit Antenna Selection for SM

The demand for high data rates in multimedia services, which requires scheme with improved error performance coupled with very high spectral efficiency. This will in turn increase the CC of the system as the spectral efficiency increases, due to the increase in the number of required transmit antennas [18]. TAS has been beneficial in SM system, as it further reduces hardware complexity and cost, achieving diversity gain.

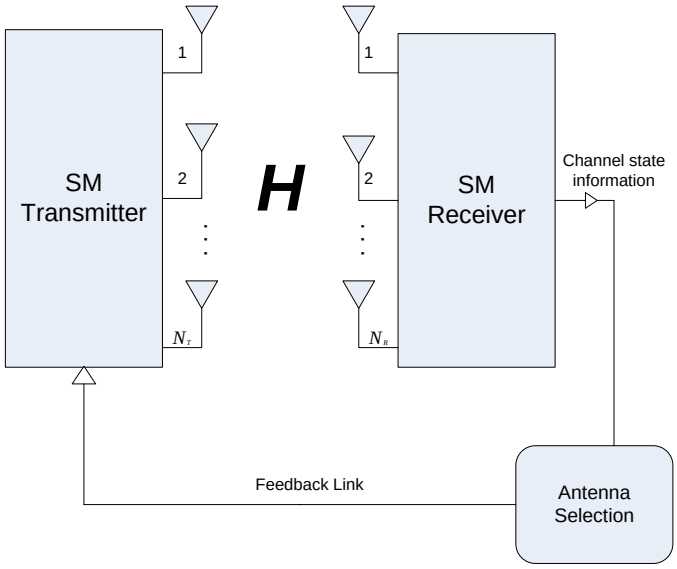

Figure 1-2 System model for low-complexity Euclidean distance transmit antenna selection [19].

The application of TAS, a transmit diversity technique is used in SM system to achieve considerable improvement in error performance. For instance, Euclidean distance based antenna selection (EDAS) was investigated in SM [20, 21], taking advantage of the ICI and IAS free property of SM and separating the QAM signal sets to further improve the error performance of the system. However, a further reduced CC version of this approach was proposed by Rajashekar *et al.* and investigated in [22], employing the approach of only one search across symmetrical constellation sets making SM practically implementable.

Recently, researchers announced the new achievement made in low-complexity transmit antenna selection (LCTAS). In [23], a low-complexity technique for both detection and antenna selection for SM was presented, employing maximum gain transmit antenna selection (MG-TAS) to reduce the average energy consumption in the system by calculating the channel gains and choosing the channel with the minimum gain for transmission.

In [19], a LCTAS was proposed by Pillay *et al.*, where channel amplitude and antenna correlation are used to select the best channel prior to transmission. The scheme exhibits a very low CC when compared to EDAS-SM. Hence, this yields a highly realizable MIMO scheme with reduced CC, making SM more realizable. An algorithm based on both schemes will be further explained/discussed in Chapter 4 of this dissertation.

1.3.3.4 Generalized Spatial Modulation

In addition, a multiple active transmit antenna scheme for generalized spatial modulation (MA-GSM) was proposed in [24] to reduce the CC of the novel GSM system which requires a high number of transmit antennas to achieve high data rate. The proposed MA-GSM uses multiple transmit antennas to convey different information at each time slot similar to the conventional SM system. Significant improvement was achieved in terms of CC in the proposed system as 10 b/s/Hz, QPSK system which requires 8 transmits antennas in conventional GSM system and 64 antennas in SM system requires only 4 transmit antennas in MA-GSM system, thus, improving the high CC with respect to high data rate.

1.3.3.5 Link Adaptation

To construct schemes with full-rate, full-diversity with spatial multiplexing such as V-BLAST, which can give high multiplexing gain for more than two transmit antennas with linear CC is impossible [24]. Likewise, It has been stated in literature that link adaptation can improve the reliability of a MIMO system [25, 26].

The process of adapting the error correction with the modulation scheme according to the condition of the link at that instant to achieve high efficiency in the system is called link adaptation [27]. Such that with a very good link, a highly efficient modulation scheme is employed and vice versa.

1.3.3.5.1 Adaptive Spatial Modulation

Adaptive SM (ASM) was investigated in [26], with maximum-likelihood (ML) based detector, which searches over the entire signal space to obtain better system performance using the CSI estimated by the receiver as a decision metric to select the optimum candidate for transmission.

Likewise, link adaptation for SM was investigated in [28], using power allocation algorithm by shrinking the error vector space and exploiting only the Euclidean distance of the dominant error vectors to optimize the power allocation matrix solving the effect of power imbalance stated in [29].

Another approach of link adaptation was investigated in [30], using pre-processing pre-coder formulation technique at the transmitter prior to transmission to achieve transmit diversity. This is done by maximizing the minimum Euclidean distance among the pre-coded codewords. Thus, improving the error performance of the system with reduced CC.

A similar approach to [30] was proposed in [31], employing two different transmit pre-coding algorithm. One is based on maximizing the minimum Euclidean distance between the SM

constellation points at the receiver as against among the codewords in [30]. The second algorithm in [31] is based on minimizing the bit error rate (BER) of SM which can jointly maximize the overall Euclidean distance between the received signal points. The Monte Carlo simulation results show that the second algorithm proposed in [31] (using minimum BER) achieved significant improvement when compared to the first algorithm (maximizing the minimum Euclidean distance) and power allocation algorithm stated earlier [28].

However, in [26], an approach similar to [31] was employed to improve the error performance using a CSI estimated by the receiver as a decision metric to select the mode with the least bit error rate (BER) as the transmitting mode. Different transmission candidate modes with the same target spectral efficiency coupled with LCTAS was employed.

The combination of two transmit diversity schemes link adaptation and TAS was employed in [26] to decrease the extreme high CC in [25]. This employs different transmission candidate modes with the same target spectral efficiency. The decision metric in [25, 26], is based on selecting the transmission candidate mode that maximizes the minimum Euclidean distance as the transmission mode at that instant.

In all the techniques discussed so far, significant improvement was achieved either in error performance or reduction in CC and at times with increased data rate. The CC in the decision metric in [25] was reduced in [26]. Similarly, in [31], the CC imposed on the system can be further reduced by employing a decision metric, which can adopt a lookup table (LUT) computation technique [32].

In this dissertation, we proposed a low CC decision metric, to achieve a lower CC in the system, computing the instantaneous bit error probability (IBEP) and the transmission candidate mode with the minimum IBEP is selected as the transmission mode. Capitalizing on the LUT computation technique and assuming the full knowledge of the channel is known at the receiver.

Likewise, a sub-optimal transmit antenna selection proposed in [19, 23] is employed to further reduce the CC by evaluating the channel amplitude and antenna correlation to eliminate the worse channel at that instant. We aim at maximizing the advantage of free ICI and IAS in the system and decreasing the CC in joint detection at the receiver. This will be discussed in details in Chapter 4 in this dissertation.

The second limitation of SM mentioned in Section 1.3.3.1, of its data rate enhancement being proportional to logarithm base-two of the total transmit antennas unlike other spatial multiplexing techniques, such as V-BLAST, whose data rate increases linearly with the number

of transmit antennas was improved on by further decomposing the spatial dimension into in-phase and quadrature-phase components [33].

This brought about an enhanced spectral efficiency form of SM called quadrature spatial modulation (QSM) [33, 34]. This will be further discussed in next sub-section and Chapter 3 of this dissertation.

1.3.3.6 Improved Spectral Efficiency for SM

QSM, an SM-based scheme, uses transmit antennas in an innovative manner to enhance the performance and throughput of the conventional SM system by using an extra spatial dimension called the quadrature-phase dimension. The spatial constellation of QSM is extended into in-phase and quadrature-phase dimensions. In QSM, the first dimension (in-phase) transmits the real part of the decomposed constellation symbol, while the second dimension (quadrature-phase) transmits the imaginary part.

In the same way, ICI and IAS are avoided completely in QSM due to symbols being orthogonal and modulated into the cosine and sine carriers, respectively [33]. This approach improves the criticism of SM by using an additional logarithm base two of the total transmit antennas. Significant improvement was achieved in QSM when compared to a conventional SM system of the same spectral efficiency [33, 34]. This will be more elaborated on in Chapter 3 of this dissertation.

1.4 Research Motivation and Problem Statement

MIMO systems have been investigated in numerous papers as the future of wireless communication scenario [1]. Recent studies have led to the development of an innovative scheme of MIMO systems called SM [15], which employs the spatial dimension to convey additional information and requires only a single RF chain for transmission, avoiding IAS and ICI completely.

The criticism of SM, of its data rate enhancement increasing only in logarithm base-two of the total number of transmit antennas compared to other spatial multiplexing techniques, brought about an enhanced spectral efficiency of SM called QSM.

QSM proposed in [33, 34], extends the spatial constellation dimension to the in-phase and quadrature-phase dimensions, which are modulated into the cosine and sine carriers, respectively, to eliminate IAS and ICI completely. QSM improves the spectral efficiency of SM by considering the additional spatial dimension (quadrature-phase) to convey information.

Significant improvement in terms of data rate was achieved in QSM when compared to a conventional SM system [33].

In [33], the overall bit error probability of QSM was derived using an asymptotic tight union bound, which does not match at the low SNR region. In [7], the overall bit error probability of SM was derived using a lower bound approach. Result shows that the approach in [7] matches very closely at lower SNR validating the results from low SNR to high SNR region than the approach employed in [33], which employs an asymptotic tight union bound. This motivates for the formulation of the theoretical analysis of QSM using a lower bound approach to validate the Monte Carlo simulation results.

The similarity and attractive features of SM and QSM include avoidance of ICI and IAS, which formed the major limitation of conventional MIMO systems. QSM exhibits significant improvement when compared to a conventional SM of the same spectral efficiency [15, 33]. In addition, link adaptation has been stated in literature that, it can further improve the error performance of a MIMO system. As investigated in [25, 26, 35], which demonstrates that link adaptation in MIMO system can further improve the error performance of the system.

In this dissertation, we propose an algorithm that employs different candidate transmission mode depending on the condition of the transmission link, such that with a very good link a highly efficient modulation scheme is employed and vice versa. The proposed scheme is called adaptive quadrature spatial modulation (AQSM).

Similarly, incorporating an optimal TAS investigated in [22] to the proposed system to further improve the error performance, imposed a high CC to the system. However, LCTAS as proposed by Pillay *et al.* [19], employing a metric of the larger the amplitude of the channel the better it is and discarding the transmit antenna based on high correlation to reduce the CC in the joint detection at the receiver. Thereby, computing the channel amplitude and antenna correlation prior to transmission to eliminate the worse channel at each transmission instant. The CC of the TAS proposed in [22] is high compared to the technique proposed in [19]. This demonstrates a very low CC as shown in the CC analysis in [19].

The decision metric in the link adaptation technique employed in [25] impose a very high CC in the system as compared to the decision metric employed in [26]. However, the CC in the decision metric in [26] and [31] can be reduced employing LCTAS using channel amplitude and antenna correlation [19]. This can be combined with link adaptation technique using a similar approach to [26], but with a decision metric of the minimum IBEP to select the transmission mode. Capitalizing on the LUT computation technique that can be adopted, this motivates the application of link adaptation in QSM system.

1.5 Research Objectives

The following are the objectives of this research:

1. Formulation of the average bit error probability for QSM system using a lower bound approach, which gives a better match across the SNR range.
2. Formulation of AQSM in terms of IBEP using a lower bound approach.
3. Investigation of an optimal TAS in the proposed AQSM system.
4. Investigation of LCTAS in the proposed AQSM system.

1.6 Organisation of Dissertation

The rest of the dissertation is organized as follows:

Chapter 2 provides a detailed description of SM, together with the numerical results.

Chapter 3 presents the system model of QSM with the performance analysis using a lower bound and asymptotic union bound approach in i.i.d frequency-flat Rayleigh fading channels to validate the Monte Carlo simulation results.

Chapter 4 introduces the proposed AQSM system with the claimed advantages of the system in terms of error performance and CC comparisons with the conventional QSM system of the same spectral efficiency. The derivation of the IBEP of the proposed scheme is presented in this chapter.

Chapter 5 concludes the dissertation and discusses possible future research directions.

1.7 Major Contribution of the Research

The work in this dissertation is ready to be submitted as a journal paper for review with the following details:
S. Oladoyinbo, N. Pillay, H. Xu "Adaptive Quadrature Spatial Modulation" [*Ready for submission to IET Communications Journal*].

The subject matter of this paper is covered in:

1.7.1 Study and Performance Analysis of QSM

The study and performance analysis of QSM using both the asymptotic union bound and a lower bound approach is presented in chapter 3.

1.7.2 Link Adaptation for QSM

Investigation of link adaptation in the QSM scheme, employing the minimum IBEP as the decision metric coupled with the study of the effect of optimal TAS and LCTAS on AQSM is presented in chapter 4.

1.8 Notation used in the Dissertation

Bold italics symbols denote vectors/matrices, while regular letters represent scalar quantities. $[\cdot]^T, (\cdot)^H, |\cdot|, \|\cdot\|_F$ and $(\cdot)^*$ represents transpose, Hermitian, Euclidean norm, Frobenius norm and complex conjugate of a number, respectively. $Q(\cdot)$ represents the Gaussian Q-function, $E\{\cdot\}$ is the expectation operator, $Re\{\cdot\}$ is the real part of a complex value, while $Im\{\cdot\}$ is the imaginary part of a complex value. $\underset{w}{\text{argmin}}(\cdot)$ represents the minimum value of an argument with respect to w, while $\underset{w}{\text{argmax}}(\cdot)$ represents the maximum value of an argument with respect to w, $\binom{\cdot}{\cdot}$ represents the binomial coefficient and i represents a complex number.

CHAPTER 2

Spatial Modulation

2 Introduction

The use of multiple antennas in an innovative manner in MIMO systems has helped in making MIMO more realizable by enhancing MIMO systems in terms of reliability and a decrease in hardware complexity [18].

Several MIMO systems have been studied comprehensively, such as SM [15], a single stream MIMO scheme, which uses the spatial (antenna) dimension to convey additional information. In SM, relatively high multiplexing gain is achieved with the major limitation of IAS and ICI experienced in conventional MIMO systems completely avoided [15, 16].

SM offers an excellent way to exploit spatial multiplexing by dividing the input bit stream into two parts; the first part is used to select one active transmit antenna from the array of transmit antennas available in the system, while the second part is mapped into an APM constellation. The modulated signal is sent out via the active transmit antenna, i.e. the selected transmit antenna.

Similarly, only a single RF chain is required in SM, as only one transmit antenna out of the available transmit antennas is used for transmission at each time slot, making the system more energy-efficient [16]. SM is presented in this dissertation as a benchmark for the proposed scheme.

2.1 Transmission Model of Spatial Modulation

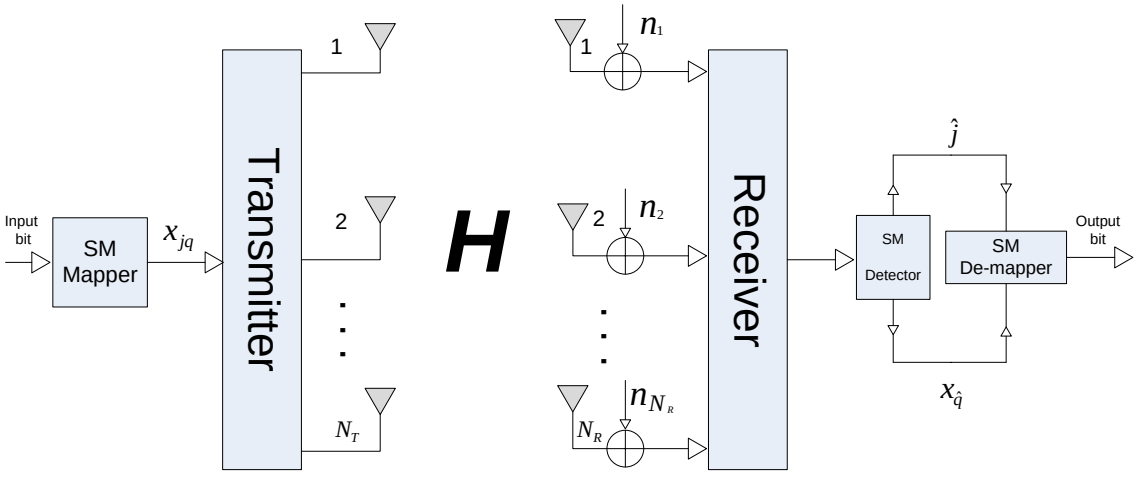

Figure 2-1 System model for Spatial Modulation [7].

Figure 2-1 illustrates an example of an SM system with N_T and N_R representing the number of transmit antennas and receive antennas, respectively. SM maps its input bit streams into an M-QAM symbol $x_q, q \in [1:M]$ and a specific antenna index $j, j \in [1:N_T]$ to convey information. Hence, the spectral efficiency of SM is defined in [7] as $m = \log_2(MN_T)$.

The process of mapping the antenna index j and symbol x_q is defined by an SM mapping table. An example of the mapping process for SM system is tabulated in Table 2-2, using a Gray-coded constellation points described in Table 2-1.

Table 2-1 Gray-coded constellation points for 4-QAM modulation order.

Input Bits ($\log_2 M$)	M-QAM Symbol
[0 0]	1+i
[0 1]	-1+i
[1 0]	-1-i
[1 1]	1-i

Table 2-2 Mapping process for 2×4 4-QAM SM system.

Input Bits	Antenna Index j	Symbol x_q	Transmitted Signal $\boldsymbol{x}_{jq}$
0 0 0	[0] = 1	[0 0] = 1+i	[1+i 0]
0 0 1	[0] = 1	[0 1] = -1+i	[-1+i 0]
0 1 0	[0] = 1	[1 0] = -1-i	[-1-i 0]
0 1 1	[0] = 1	[1 1] = 1-i	[1-i 0]
1 0 0	[1] = 2	[0 0] = 1+i	[0 1+i]
1 0 1	[1] = 2	[0 1] = -1+i	[0 -1+i]
1 1 0	[1] = 2	[1 0] = -1-i	[0 -1-i]
1 1 1	[1] = 2	[1 1] = 1-i	[0 1-i]

In the Table 2-2, a 2×4 4-QAM SM system is considered, with a spectral efficiency of 3 b/s/Hz. The first bit activates the antenna index j and the last two bits select the symbol x_q.

The mapped bits are transmitted via a single transmit antenna j, which was activated by the antenna index.

The transmit vector of the scheme is expressed as [7]:

$$\boldsymbol{x}_{jq} = \underset{1^{st}\text{ Position}}{\uparrow}\underset{}{[0}\ 0\ \ldots\ \underset{j^{th}\text{ Position}}{\underset{\downarrow}{x_q}}\ \ldots\ \underset{N_T^{th}\text{Position}}{\underset{\uparrow}{0}}]^T \tag{2-1}$$

Considering a 2×4 4-QAM SM system with $m = 3$ b/s/Hz, first, $\log_2(N_T)$ is used to select the active transmit antenna out of the two available transmit antennas. Likewise, $\log_2(M)$, is used to modulate the 4-QAM constellation symbol x_q. The transmit vector $\boldsymbol{x}_{jq}$ of dimension $N_T \times 1$ is transmitted via the selected active transmit antenna j over channel $\boldsymbol{H}$ of i.i.d entries with dimension $N_R \times N_T$ with $CN\ (0,1)$ distribution, experiencing AWGN $\boldsymbol{n}$ of $N_R \times 1$ dimension, with i.i.d entries of $CN\ (0,1)$ distribution, such that the received signal $\boldsymbol{y}$ becomes:

$$\boldsymbol{y} = \sqrt{\rho}\boldsymbol{H}\boldsymbol{x}_{jq} + \boldsymbol{n} \tag{2-2}$$

where ρ is the average SNR at each receive antenna.

Assuming the j^{th} antenna is used for transmission, the received signal can be rewritten as:

$$\boldsymbol{y} = \sqrt{\rho}\boldsymbol{h}_j\boldsymbol{x}_{jq} + \boldsymbol{n} \tag{2-3}$$

where $j \in [1: N_T]$, $q \in [1: M]$ and ρ denotes the average SNR and $\boldsymbol{h}_j$ is the j^{th} column of the channel $\boldsymbol{H}$.

An estimate of the transmit antenna index with the estimated modulated symbol are detected optimally using ML at the receiver to demodulate the transmitted signal, assuming the full knowledge of the channel is known at the receiver. Optimal detection for SM will be discussed in the next sub-section.

2.1.1 Optimal Detection for Spatial Modulation

The transmitted signal is detected at the receiver by estimating the transmit antenna index j used for transmission and the modulated symbol x_q by searching the whole signal space M

constellation points and N_T transmit antennas, i.e. ($N_T M$). Since, SM encodes data to its antenna index and the modulated symbol [16].

The estimates are then fed into the SM de-mapper to recover the transmitted bits, using the SM mapping table (Table 2-1 and Table 2-2) in a reverse mapping process. ML approach is employed to jointly detect the transmitted symbol and the antenna index. This is given as [7, 16]:

$$[k, x_{\hat{q}}] = \underset{q \in [1:M]}{\operatorname{argmin}} \left(\left\| \boldsymbol{y} - \sqrt{\rho} \boldsymbol{H} x_q \right\|_F^2 \right) \tag{2-4}$$

$$[k, x_{\hat{q}}] = \underset{q \in [1:M]}{\operatorname{argmax}} \left(\sqrt{\rho} \left\| \boldsymbol{g}_{jq} \right\|_F^2 - 2Re\{\boldsymbol{y}^H \boldsymbol{g}_{jq}\} \right) \tag{2-5}$$

where $\boldsymbol{g}_{jq} = \boldsymbol{h}_j x_{\hat{q}}$ and is the transmit antenna index and the estimated transmitted symbol, respectively.

2.2 Performance Analysis for Spatial Modulation

The performance analysis for the average BER ML-based SM, was derived in closed-form expression in [16]. The analysis in [16] is only applicable to binary phase shift keying (BPSK) modulation. However, in [7, 8], the theoretical analysis for square M-QAM SM was derived in closed-form expression to quantify the average BER performance of the system.

In this section, a lower bound approach is employed to compute the theoretical analysis for SM similar to [8], considering the symbol estimation error and antenna index estimation error independently.

In [8], the overall probability of error for SM is given as:

$$P_e = P_a + P_d - P_a P_d \tag{2-6}$$

where P_a is the bit error probability of the antenna index considering that the symbol is perfectly detected, while P_d is the bit error probability of the estimated symbol considering that the antenna index is perfectly detected.

2.2.1 Analysis of Symbol Estimation

In [8, 36], the average symbol error rate (SER) for M-QAM over a Rayleigh fading channel is given as:

$$\mathrm{SER}(k) = \left(\frac{a}{c}\left[\frac{1}{2}\left(\frac{2}{bp+2}\right)^{Nr} - \frac{a}{2}\left(\frac{1}{bp+1}\right)^{Nr} + (1-a)\sum_{i=1}^{c-1}\left(\frac{2sin^2\theta}{bp+2sin^2\theta}\right)^{Nr} + \sum_{i=c}^{2c-1}\left(\frac{2sin^2\theta}{bp+2sin^2\theta}\right)^{Nr}\right]\right) \quad (2\text{-}7)$$

where $a = 1 - \frac{1}{\sqrt{M}}$, $b = \frac{3}{M-1}$, $\theta = \frac{i\pi}{4c}$ and $c > 10$, and the BER at high SNR is given by:

$$P_d \cong \frac{SER}{m} \quad (2\text{-}8)$$

where $m = \log_2 M$.

2.2.2 Analysis of Transmit Antenna Index Estimation

The bit error probability of the transmit antenna index is computed similar to [7, 8]. According to [7], the transmit antenna index is union bounded by:

$$P_a(k) \leq \frac{1}{Nt \times M \times log_2(Nt)} \sum_{q=1}^{M} \sum_{\hat{j}=1}^{Nt} \sum_{j=1}^{Nt} N(j,\hat{j})\, \mathrm{P}\left(\boldsymbol{x}_{jq} \rightarrow \boldsymbol{x}_{\hat{j}q}\right) \quad (2\text{-}9)$$

where $\mathrm{P}\left(\boldsymbol{x}_{jq} \rightarrow \boldsymbol{x}_{\hat{j}q}\right)$ is the pairwise error probability (PEP) of choosing $x_{\hat{j}q}$, given that x_{jq} was transmitted. $N(j,\hat{j})$ is the number of bit errors between the transmitted antenna index j and the estimated transmit antenna index $\hat{j}$.

The closed-form of the conditional PEP of the channel matrix $\boldsymbol{H}$ is given in [7] as:

$$\mathrm{P}(\boldsymbol{x}_{jq} \to \boldsymbol{x}_{\hat{j}q}|\boldsymbol{H}) = P\left(\|\boldsymbol{y} - \sqrt{\rho}\boldsymbol{h}_{\hat{j}}x_q\|_F < \|\boldsymbol{y} - \sqrt{\rho}\boldsymbol{h}_j x_q\|_F\right) = Q(\sqrt{\gamma}) \qquad (2\text{-}10)$$

Using $Q(x) = \frac{1}{\pi}\int_0^{\pi/2} \exp\left(-\frac{s^2}{2\sin^2\theta}\right) d\theta$ and solving for $P_\gamma = \int_0^\infty Q(\sqrt{\gamma})\, d\gamma$, the closed-form of (2-10) can be verified to be the same as (18) in [7]. This is formulated using integration by part with moment generating function (MGF) and the alternative form of Q-function, to get the average PEP over a joint distribution of the channel gain and this can be varied to be:

$$\mathrm{P}(\boldsymbol{x}_{jq} \to \boldsymbol{x}_{\hat{j}q}) = \mu^{Nr} \sum_{k=0}^{Nr-1} \binom{Nr-1+k}{k} [1-\mu]^k \qquad (2\text{-}11)$$

where $\mu = \frac{1}{2}\left(1 - \sqrt{\frac{\alpha}{\alpha+1}}\right)$ and $\alpha = \frac{\rho}{2}|x_q|^2$.

2.3 Numerical Analysis of the Computed Analytical and Simulated BER for Spatial Modulation

The analytical result for the conventional SM system employing a lower bound approach is computed in this section to validate the Monte Carlo simulation results. The result presented in Figure 2-2 is equipped with two transmit antennas coupled with four and two receive antennas, respectively, employing 4-QAM. The analytical result validates the Monte Carlo simulation results, as they closely match from low SNR to high SNR region. It was observed that, as the number of the receive antenna increases the BER performance of the system improves as expected. At a BER of 10^{-5} the 2×4 4-QAM SM system achieves a gain of approximately 11 dB over 2×2 4-QAM SM system.

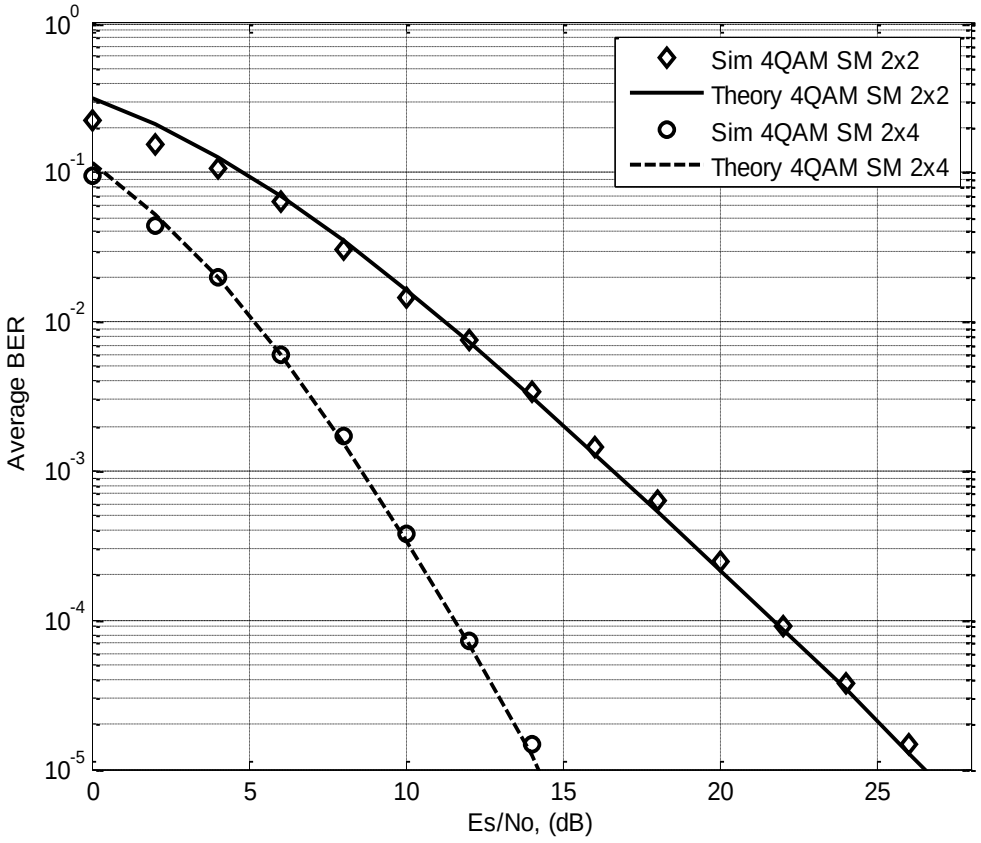

Figure 2-2 Validation of 4-QAM 2×4 and 2×2 SM theoretical analysis with the Monte Carlo simulation result

The result presented in Figure 2-3, is equipped with two transmit antennas coupled with four and two receive antennas, respectively, employing 16-QAM. The theoretical result validates the Monte Carlo simulation results. At a BER of 10^{-5} the 2×4 16-QAM SM system achieves a gain of approximately 10 dB over 2×2 16-QAM SM system.

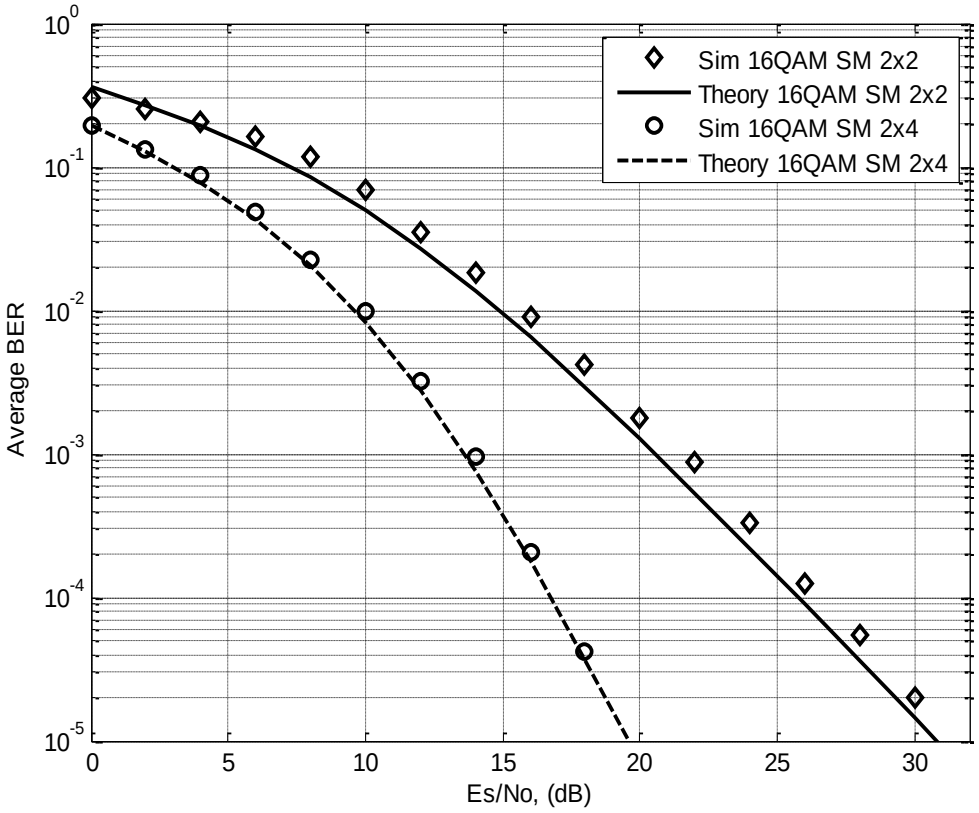

Figure 2-3 Validation of 16-QAM 2 × 4 and 2 × 2 SM theoretical analysis with the Monte Carlo simulation result

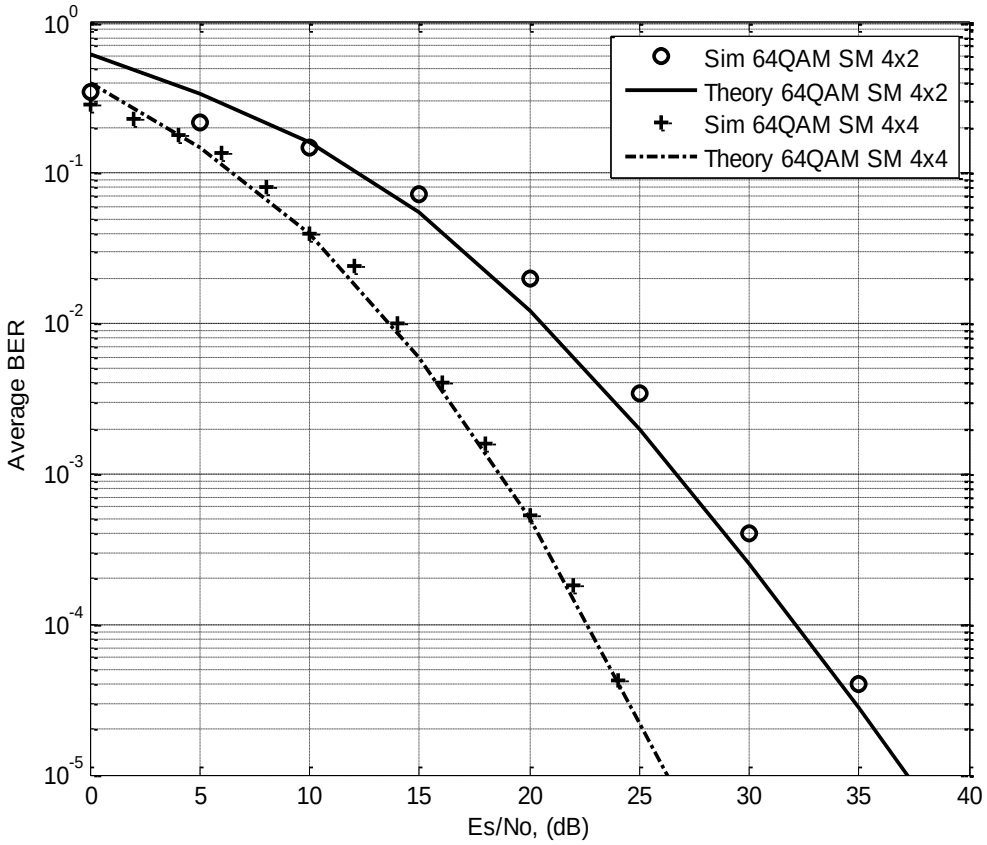

Figure 2-4 Validation of 64-QAM 4×4 and 4×2 SM theoretical analysis with the Monte Carlo simulation result

In Figure 2-4, at a BER of 10^{-5} the 4×4 64-QAM SM system achieves a gain of approximately 10 dB over 4×2 64-QAM SM system, with the theoretical result validating the Monte Carlo simulation results from low SNR to high SNR region.

2.4 Chapter Summary

The system model of a conventional SM system with an optimal detector was presented in this chapter. Similarly, the average BER for M-QAM SM system with optimal detector over an i.i.d Rayleigh fading channels $\boldsymbol{H}$ quantify with the formulated theoretical analysis validating the Monte Carlo simulation results. The analytical framework is shown to be relatively tight with the simulated BER of the SM system as shown in Figure 2-2, 2-3 and 2-4, respectively.

CHAPTER 3

Quadrature Spatial Modulation

3 Introduction

The criticism of SM, of its data rate enhancement increasing only in logarithm base-two of the total number of transmit antennas compared to other spatial multiplexing techniques, brought about an enhanced spectral efficiency of SM called QSM.

High data rates are highly desirable in wireless communication, but an increase in data rates requires additional transmit antennas, which is expensive. In addition, an increase in the number of required transmit antennas will result to high CC. MIMO systems can achieve high spectral efficiencies with good system reliability [1, 8], this has drawn attention to the system over the years resulting in the use of multiple transmit antennas in an innovative manner to achieve high spectral efficiencies.

In SM [15], a high spectral efficiency is achieved by employing spatial dimension to convey information. Although, SM has a criticism of its data rate being proportional to the logarithm base-two of the number of transmit antennas, when compared to V-BLAST, whose data rate increases linearly with N_T. In improving this criticism, an enhanced spectral efficiency SM called QSM was proposed by Mesleh *et al.* [33].

QSM, adds an additional dimension to its modulation spatial dimension, i.e. the spatial dimension is extended to the in-phase and quadrature-phase dimensions to enhances the overall spectral efficiency of the system [34]. The constellation symbols are further decomposed into real and imaginary components, while the first dimension transmits the real part of the constellation symbol and the imaginary part is transmitted via the second dimension.

Furthermore, IAS and ICI are completely avoided considering that the in-phase and quadrature-phase components of the constellation symbols are modulated into the cosine and sine carriers, respectively [33, 34].

The features of QSM are summarized as follows:

1. QSM improves the criticism of SM with enhanced spectral efficiency with respect to number of transmit antennas [33].
2. In QSM, a single RF chain is employed. Likewise, ICI and IAS are avoided considering the in-phase and quadrature-phase components of the symbol are modulated into the cosine and sine carriers, respectively [33].

3.1 System Model of Quadrature Spatial Modulation

Figure 3-1, depicts a detailed QSM system model equipped with N_T transmit antennas and N_R receive antennas.

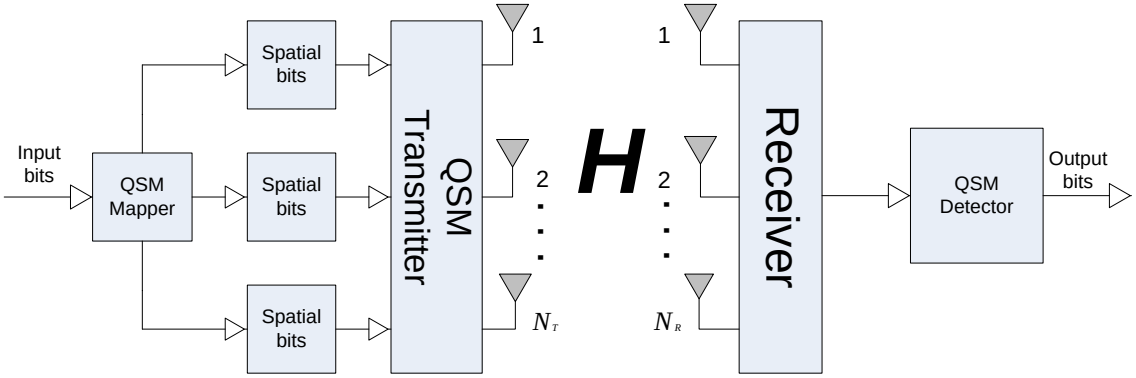

Figure 3-1 System model for quadrature spatial modulation [37]

In the QSM system [33] and [34], the spectral efficiency $m = \log_2(MN_T^2)$, where M is the modulation order and N_T is the total number of transmit antennas. The M-QAM constellation symbol $x_q, q \in [1:M]$ is modulated by $\log_2 M$ bits and $\log_2 N_T$ bits are used to select the active transmit antenna to transmit the real part of the constellation symbol, while an additional $\log_2 N_T$ bits are used to select the second transmit antenna to transmit the imaginary part of the constellation symbol. Hence, $2\log_2 N_T$ bits are required to select the active antenna indices needed to transmit the constellation symbol per transmission instant.

The modulated symbol $x_q = x_{Re}^q + ix_{Im}^q$ is further decomposed into real and imaginary components, while the real part of the modulated symbol x_{Re}^q is transmitted via one of the selected active transmit antenna index j_R and the imaginary part of the modulated symbol x_{Im}^q is transmitted via the second transmit antenna index j_I.

An example of the mapping process for QSM system is tabulated in Table 3-1:

Table 3-1 Mapping process of QSM system.

Configuration	Input Bits $\log_2 MN_T^2$	First $\log_2 M$ bits	Second $\log_2 N_T$ bits	Third $\log_2 N_T$ bits
$M = 4$ $N_T = 2$ $N_R = 4$	0 0 0 1	$\log_2 4 = 2$ bits [0 0] $x_q = -1 + i$ $x_{Re}^q = -1$ $x_{Im}^q = +i$	$\log_2 2 = 1$ bit [0] $j_R = 1$	$\log_2 2 = 1$ bit [1] $j_I = 2$
$M = 4$ $N_T = 4$ $N_R = 4$	1 1 0 1 0 0	$\log_2 4 = 2$ bits [1 1] $x_q = +1 - i$ $x_{Re}^q = +1$ $x_{Im}^q = -i$	$\log_2 4 = 2$ bits [0 1] $j_R = 2$	$\log_2 4 = 2$ bits [0 0] $j_I = 1$
$M = 16$ $N_T = 4$ $N_R = 4$	1 0 0 1 1 1 0 1	$\log_2 16 = 4$ bits [1 0 0 1] $x_q = +3 + i$ $x_{Re}^q = +3$ $x_{Im}^q = +i$	$\log_2 4 = 2$ bits [1 1] $j_R = 4$	$\log_2 4 = 2$ bits [0 1] $j_I = 2$

In the Table 3-1, a 2×4 4-QAM QSM system is considered, with a spectral efficiency of 4 b/s/Hz. The first two bits select the symbol x_q, while the third bit activates the antenna index j_R to transmit the real component of the symbol x_{Re}^q and the fourth bit activates the antenna index j_I to transmit the imaginary component of the symbol x_{Im}^q.

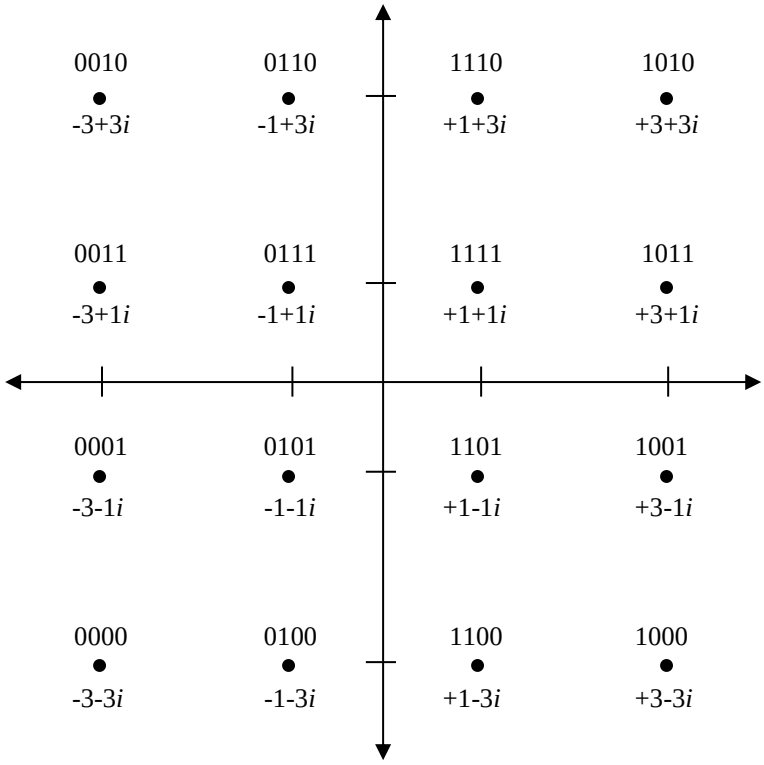

Figure 3-2 16-QAM constellation points

The transmitted symbol x_q, which is the combination of x_{Re}^q and x_{Im}^q of dimension $N_T \times 1$ is transmitted via a Rayleigh frequency-flat fading channel $\boldsymbol{H}$ of dimension $N_R \times N_T$ with i.i.d entries and $CN(0,1)$ distribution, experiencing $N_R \times 1$ dimension of AWGN $\boldsymbol{n}$ with $CN(0,1)$ distribution.

Note that, when a single transmit antenna is used, i.e. the antenna indices to select the active transmit antennas to transmit both the real and imaginary part of the constellation symbol are the same, such that, $x_q = x_{Re}^q + ix_{Im}^q$. Thus, the received signal vector $\boldsymbol{y}$ becomes:

$$\boldsymbol{y} = \sqrt{\rho}\boldsymbol{h}_\ell x_q + \boldsymbol{\eta}, \ell \in [1: N_T], q \in [1: M] \quad (3\text{-}1)$$

where ρ is the average SNR and ℓ is the corresponding transmit antenna index.

Assuming both the ℓ^{th} antenna is used to transmit the real and imaginary part of the symbol, the received signal can be rewritten as:

$$\boldsymbol{y} = \sqrt{\rho/_2}\, \boldsymbol{h}^1_{j_R} x^q_{Re} + i\sqrt{\rho/_2}\, \boldsymbol{h}^2_{j_I} x^q_{Im} + \boldsymbol{\eta} \tag{3-2}$$

where j_R and $j_I \in [1: N_T(N_T - 1)]$.

Note, (3-2) represents $\boldsymbol{y}$, when two transmit antennas are employed for transmission. Such that, the antenna indices to select the active transmit antennas to transmit both the real and imaginary part of the constellation symbol are different.

The received signal $\boldsymbol{y}$ is detected optimally by estimating the antenna index and the modulated symbol to recover the transmitted information. The full knowledge of the channel is assumed to be known at the receiver.

3.1.1 Optimal Detection

In this dissertation, the received signal is demodulated optimally employing ML detection, which searches the entire signal space of M constellation points and all possible antenna index combinations. This can be expressed as [33]:

$$\left[\hat{j}_R, \hat{j}_I, \hat{x}^q_{Re}, \hat{x}^q_{Im}\right] = \underset{j_R, j_I, x^q_{Re}, x^q_{Im}}{\operatorname{argmin}} \left(\left\| \boldsymbol{y} - \sqrt{\rho/_\mu}\, \left(\boldsymbol{h}^1_{j_R} x^q_{Re} + i\boldsymbol{h}^2_{j_I} x^q_{Im} \right) \right\|^2_F \right)$$

$$= \underset{j_R, j_I, x^q_{Re}, x^q_{Im}}{\operatorname{argmin}} \left\{ \|\boldsymbol{g}\|^2_F - 2Re\{\boldsymbol{y}^H \boldsymbol{g}\} \right\} \tag{3-3}$$

where $\boldsymbol{g} = \sqrt{\rho/_\mu}\, \left(\boldsymbol{h}^1_{j_R} x^q_{Re} + i\boldsymbol{h}^2_{j_I} x^q_{Im} \right)$ and $\boldsymbol{h}^1_{j_R} x^q_{Re}$, $\boldsymbol{h}^2_{j_I} x^q_{Im}$ represents the real and the imaginary parts of the complex argument, respectively.

3.2 Performance Analysis of M-QAM Quadrature Spatial Modulation using Asymptotic Tight Union Bound

The theoretical analysis for M-QAM QSM system is computed employing an upper bound approach following an asymptotically tight union bound in [33]. Similar to [33], will compute the theoretical analysis for M-QAM QSM system to validate the Monte Carlo simulation results.

Considering the received signal $\boldsymbol{y}$:

$$\boldsymbol{y} = \sqrt{\rho/2}\boldsymbol{h}_{j_R}^1 x_{Re}^q + i\sqrt{\rho/2}\boldsymbol{h}_{j_I}^2 x_{Im}^q + \boldsymbol{\eta}$$

$$\boldsymbol{g} = \sqrt{\rho/2}\boldsymbol{h}_{j_R}^1 x_{Re}^q + i\sqrt{\rho/2}\boldsymbol{h}_{j_I}^2 x_{Im}^q$$

$$\mathrm{P}(\boldsymbol{g} \to \widehat{\boldsymbol{g}}|\boldsymbol{H}) = P(\|\boldsymbol{y} - \widehat{\boldsymbol{g}}\|_F < \|\boldsymbol{y} - \boldsymbol{g}\|_F)$$

$$\mathrm{P}(\boldsymbol{g} \to \widehat{\boldsymbol{g}}|\boldsymbol{H}) = Q\left(\sqrt{k}\right) \tag{3-4}$$

where $k = \frac{\rho}{2}\left\|\boldsymbol{h}_j x_q - h_j x_q\right\|_F^2$, refer to Appendix A in [7] for derivation of k.

To get the average PEP we average (3-4) over joint probability distribution of the channel gain using MGF and the alternative form of Q-function. The PDF of the SNR over a Rayleigh fading channel is given in [38], considering one receive antenna.

The closed-form of (3-4) is given in [7] using integration by part as:

$$P_b = \mathrm{P}(\boldsymbol{g} \to \widehat{\boldsymbol{g}}|\boldsymbol{H}) = \mu^{Nr} \sum_{k=0}^{Nr-1} \binom{Nr - 1 + k}{k} [1 - \mu]^k \tag{3-5}$$

where $\mu = \frac{1}{2}\left(1 - \sqrt{\frac{\gamma/2}{\gamma/2+1}}\right)$.

In [33], γ is given as a random variable with the following mean conditions:

$$v(u) = \begin{cases} \left(\left|x_{Re}^q\right|^2 + \left|x_{\hat{R}e}^q\right|^2 + \left|x_{Im}^q\right|^2 + \left|x_{Im}^q\right|^2\right) & \text{if } \boldsymbol{h}_{j_R}^1 \neq \boldsymbol{h}_{j_R}^1, h_{j_I} \neq \boldsymbol{h}_{j_I}^2 \\ \left(\left|x_{Re}^q - x_{\hat{R}e}^q\right|^2 + \left|x_{Im}^q\right|^2 + \left|x_{\hat{I}m}^q\right|^2\right) & \text{if } \boldsymbol{h}_{j_R}^1 = \boldsymbol{h}_{j_R}^1, h_{j_I} \neq \boldsymbol{h}_{j_I}^2 \\ \left(\left|x_{Re}^q - x_{\hat{R}e}^q\right|^2 + \left|x_{Im}^q - x_{\hat{I}m}^q\right|^2\right) & \text{if } \boldsymbol{h}_{j_R}^1 = \boldsymbol{h}_{j_R}^1, h_{j_I} = \boldsymbol{h}_{j_I}^2 \\ \left(\left|x_{Re}^q\right|^2 + \left|x_{\hat{R}e}^q\right|^2 + \left|x_{Im}^q - x_{\hat{I}m}^q\right|^2\right) & \text{if } \boldsymbol{h}_{j_R}^1 \neq \boldsymbol{h}_{j_R}^1, h_{j_I} = \boldsymbol{h}_{j_I}^2 \end{cases} \tag{3-6}$$

$$\gamma = \frac{\rho}{2} v(u)\sigma^2(u) \quad \text{for } \sigma = 1 \text{ then, } \gamma = \frac{\rho}{2} v(u) \tag{3-7}$$

In [33], the asymptotic tight union bound is given as:

$$\text{ABER} = \frac{1}{N_T^2 M} \sum_{n=1}^{2^m} \sum_{k=1}^{2^m} \frac{1}{m} \times P_b \times N(j, \hat{j}) \tag{3-8}$$

where j is the antenna index used for transmission and $\hat{j}$ is the estimated antenna index, such that $N(j, \hat{j})$ is the number of bit errors associated with the corresponding PEP event.

The computed upper bound approach validates the Monte Carlo simulation results, with little variation at the lower SNR. However, in [7], the computed performance analysis for M-QAM SM using a lower bound approach shows a better validation of the Monte Carlo simulation results from low SNR to high SNR region as seen in Figure 3-3, 3-4, 3-5, respectively. This motivates for the derivation of the performance analysis for QSM system employing the lower bound approach of [7] to validate the Monte Carlo simulation results.

3.3 The Proposed Performance Analysis for M-QAM Quadrature Spatial Modulation

Similar to [7], the theoretical analysis for square M-QAM QSM system is derived using a lower bound approach showing a very close match/validation at the lower SNR.

The theoretical analysis for QSM system using the lower bound approach is computed as:

$$\begin{aligned} P_e &\geq 1 - ((1 - P_a)(1 - P_b)) \\ &= P_a + P_b - P_a P_b \end{aligned} \tag{3-9}$$

where P_a is the bit error probability of the antenna index given that symbol is perfectly detected and P_b is the bit error probability of the estimated symbol given that the antenna index is perfectly detected.

3.3.1 Analytical Average BER of Symbol Estimation

Employing a square M-QAM, the bit error probability of the symbol estimation considering the antenna index is perfectly detected, P_b can be derived similar to [7] and [36].

$$P_b = \frac{1}{\log_2 M}\left(4A_l^M(\rho) - \left(4A_l^M(\rho)\right)^2\right) \tag{3-10}$$

where $A_l^M(\rho)$= $\left(1-\frac{1}{\sqrt{M}}\right)Q\left(\sqrt{\frac{3\rho}{2(M-1)}}\right)$. Employing $\frac{\rho}{2}$ due to two transmit antennas are active at the same time to transmit the real and imaginary component of the symbol.

Substituting the alternative Q-function into P_b and using trapezoidal rule to $Q(x)$ and $Q^2(x)$ in MGF as shown in [36] for maximum ratio combiner (MRC) and Rayleigh fading channel, the close form of P_b is shown in [7] and [36] as:

$$P_b(k) = \frac{1}{\log_2 M}\left(\frac{a}{c}\left[\frac{1}{2}\left(\frac{2}{bp+2}\right)^{Nr} - \frac{a}{2}\left(\frac{1}{bp+1}\right)^{Nr} + (1-a)\sum_{i=1}^{c-1}\left(\frac{2\sin^2\theta}{bp+2\sin^2\theta}\right)^{Nr} + \sum_{i=c}^{2c-1}\left(\frac{2\sin^2\theta}{bp+2\sin^2\theta}\right)^{Nr}\right]\right) \tag{3-11}$$

where $a = 1-\frac{1}{\sqrt{M}}$, $b = \frac{3}{M-1}$, $\theta = \frac{i\pi}{4c}$ and $c > 10$.

3.3.2 Analytical Average BER of Transmit Antenna Index Estimation

Similarly, using the approach in [7] the derived bit error probability of the antenna index considering the symbol is perfectly detected P_a can be computed as:

$$P_a(k) \leq \frac{1}{Nt \times M \times log_2(Nt)}\sum_{q=1}^{M}\sum_{\hat{j}=1}^{Nt}\sum_{j=1}^{Nt} N(j,\hat{j})\,\mathrm{P}\left(\boldsymbol{x}_{jq} \to \boldsymbol{x}_{\hat{j}q}\right) \tag{3-12}$$

To get the average PEP, we average (3-12) over joint probability distribution of the channel gain using MGF and alternative form of Q-function over a Rayleigh fading channel, which is given in [38]. Using integration by part, the closed-form can be expressed as [3, 7]:

$$\mathrm{P}(\boldsymbol{x}_{jq} \to \boldsymbol{x}_{\hat{j}q}) = \mu^{Nr} \sum_{k=0}^{Nr-1} \binom{Nr-1+k}{k} [1-\mu]^k \tag{3-13}$$

where $= \frac{1}{2}\left(1 - \sqrt{\frac{\alpha/2}{\alpha/2+1}}\right)$.

Furthermore, considering the further decomposition of the constellation symbol into in-phase and quadrature-phase components and transmitted with two different transmit antennas, respectively. The antenna error of transmitting the real part and the imaginary part of the symbol is considered independently such that, $P_a = 2P_a$, considering P_a^2 is negligible given that:

$$P_a = 1 - (1 - P_a)(1 - P_a) \cong 2P_a \tag{3-14}$$

Therefore, $\alpha = \frac{\rho}{2}|x_q|^2 \times \frac{1}{2}$, due to two transmit antennas are active at the same time and the finally substitution in (3-12) becomes:

$$P_a(k) \leq \sum_{q=1}^{M} \sum_{\hat{j}=1}^{Nt} \sum_{j=1}^{Nt} \frac{N(j,\hat{j})\mu^{Nr} \sum_{k=0}^{Nr-1} \binom{Nr-1+k}{k} [1-\mu]^k}{Nt \times M \times log_2(Nt)} \tag{3-15}$$

3.4 Numerical Analysis of the Computed Analytical BER and Simulated BER for Quadrature Spatial Modulation

The analytical result of the conventional QSM system employing an asymptotic tight union bound and the proposed lower bound approach was computed to validate the Monte Carlo simulation results. The notation $N_T \times N_R$ is used to denote the number of transmit antennas and number of receive antennas, respectively.

In Figure 3-3, the system is equipped with two transmit antennas and considered under two receive antennas and four receive antennas, respectively, employing 4-QAM, i.e. 2×4 4-QAM and 2×2 4-QAM. It was observed that, the BER performances improve as the number of

receive antenna N_R increases. The 2×4 4-QAM QSM system achieves a gain of approximately 12 dB over the 2×2 4-QAM QSM system at a BER of 10^{-5}.

The analytical result obtained using a lower bound approach, validates the Monte Carlo simulation results from low SNR to high SNR region when compared to the asymptotic union bound approach, which has a wider variation at low SNR region. In Figure 3-3, the result obtained for the configuration of $N_R = 4$, employing the asymptotic union bound approach has a variation of approximately 2 dB at the lower SNR as against the proposed lower bound approach, which has a variation of approximately 1.5 dB at the low SNR region.

In addition, in Figure 3-3, the result obtained for the configuration $N_R = 2$, employing asymptotic union bound approach has a variation of approximately 6 dB at the low SNR region as against the lower bound approach, which has a variation of approximately 4 dB at the lower SNR, this is tabulated in Table 3-3.

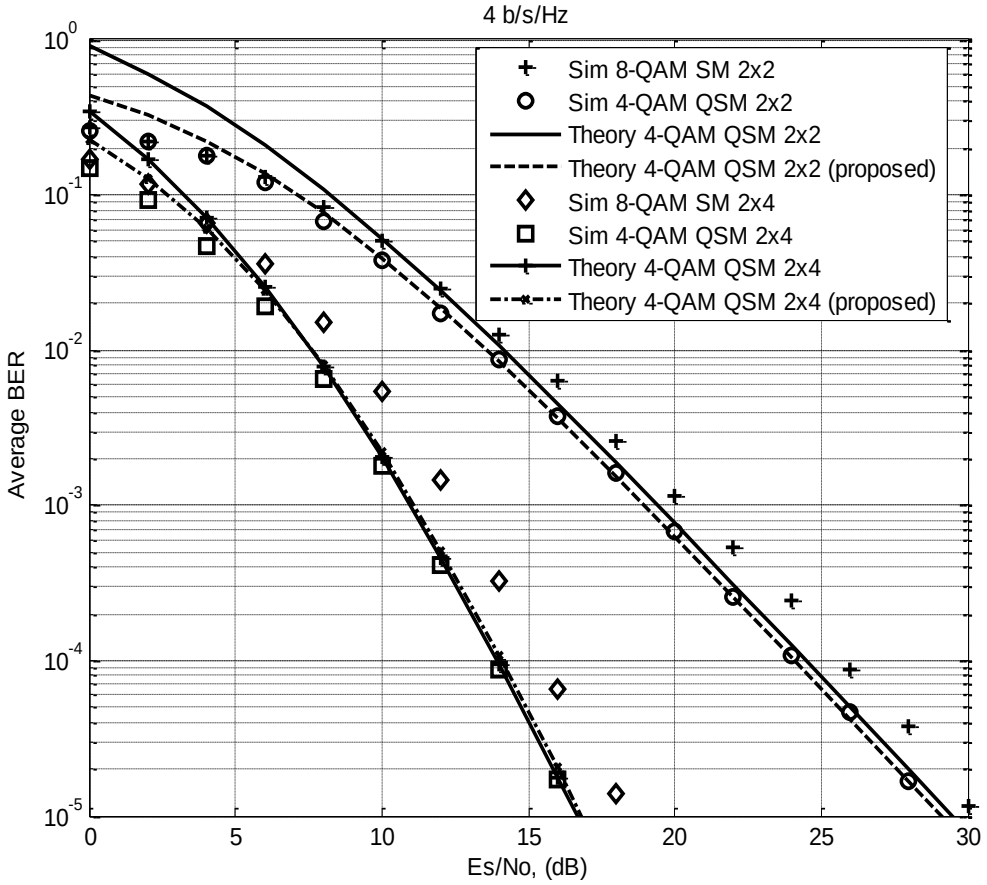

Figure 3-3 BER performance of QSM for 4 b/s/Hz.

Figure 3-4, shows two system configurations for QSM scheme, viz, 4×4 4-QAM and 4×2 4-QAM. For $N_R = 4$, the result obtained validates the Monte Carlo simulation results with variation of approximately 4 dB at the low SNR region employing the asymptotic union bound, while the lower bound approach, exhibits a variation of approximately 1.8 dB. The 4×4 4-QAM QSM system achieves a gain of approximately 13 dB over the 4×2 4-QAM QSM system at a BER of 10^{-5}.

The 4×4 4-QAM QSM system is compared with SM system of the same spectral efficiency. The QSM system exhibits a gain of approximately 3 dB over the SM system, for $N_R = 4$. Similarly, the same system settings with two receive antennas, i.e. 4×2 4-QAM QSM and 4×2 16-QAM SM system was compared and a gain of approximately 2 dB was achieved. The various gain achieved under different configuration is tabulated in Table 3-2.

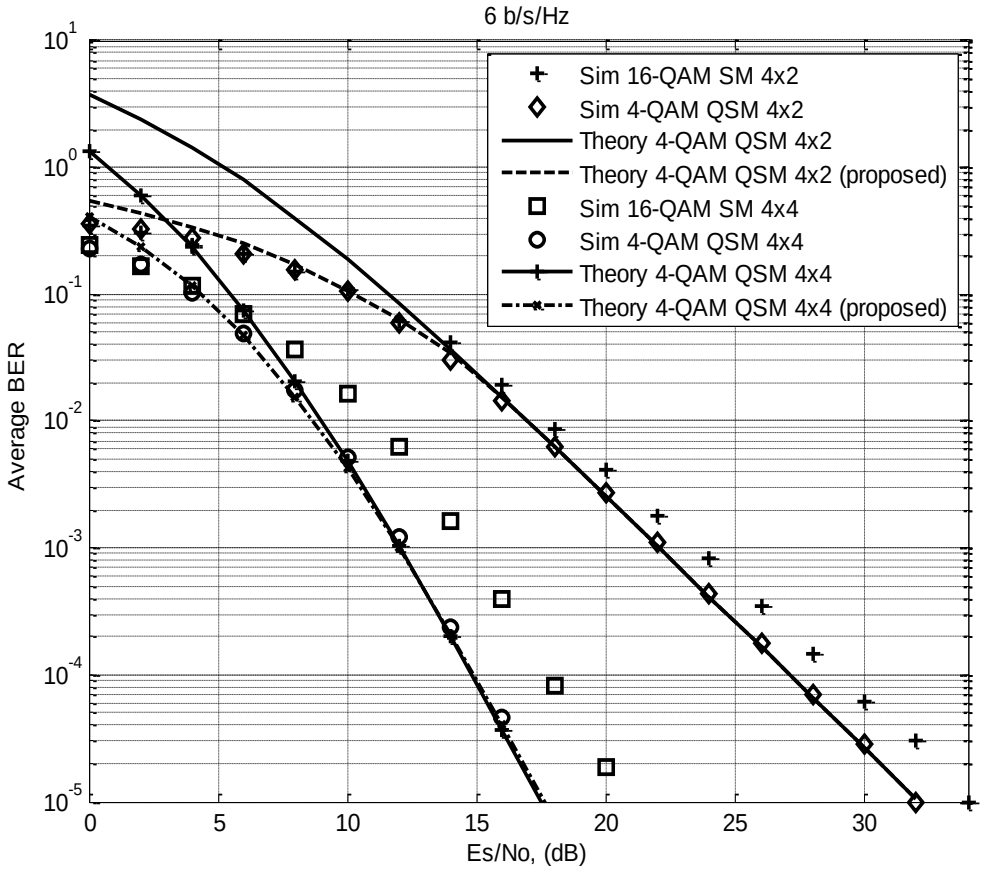

Figure 3-4 BER performance of QSM for 6 b/s/Hz.

Figure 3-5, shows a configuration for QSM system of 4×4 16-QAM and 4×2 16-QAM. It was observed that the analytical result and the Monte Carlo simulation results are both tight at

high SNR as the number of receive antenna N_R increases. Similarly, increasing the number of the receive antenna N_R, further improve the BER performance of the overall system. The 4×4 16-QAM QSM system achieves a gain of approximately 13 dB over the 4×2 16-QAM QSM system at a BER of 10^{-5}.

Figure 3-5, depicts the analytical result of QSM system employing both the asymptotic union bound and the lower bound approach. The lower bound approach achieves a better validation of the Monte Carlo simulation result with variation of approximately 3.5 dB, as against the asymptotic union bound approach, which has a variation of approximately 9 dB, considering $N_R = 4$ at the low SNR region.

Likewise, considering $N_R = 2$, the lower bound approach has a variation of approximately 6 dB, as against the asymptotic union bound approach, which has a variation of approximately 14 dB. The various variation achieved under different configuration is tabulated in Table 3-3.

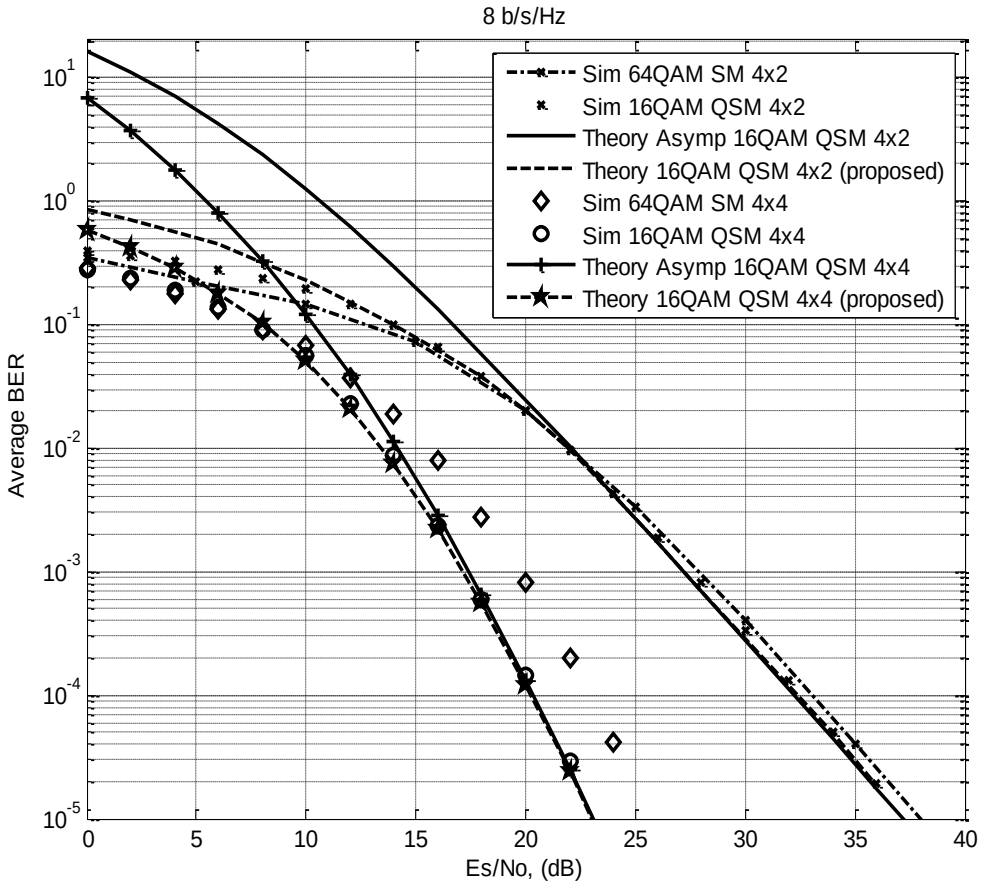

Figure 3-5 BER performance of QSM for 8 b/s/Hz

The QSM system is compared to SM system with the same spectral efficiency, the gain achieved under different configuration is tabulated in Table 3-2.

Table 3-2 SNR gain (dB) of QSM achieved over SM

Configuration	$M = 4, N_T = 2$	$M = 4, N_T = 4$	$M = 16, N_T = 4$
$N_R = 2$	1.70	2	1.2
$N_R = 4$	2	3.0	2.0

Table 3-3 SNR gain (dB) variation of lower bound approach achieved over asymptotic union bound

Configuration	Proposed Approach $N_R = 2$	Upper Bound Approach $N_R = 2$	Proposed Approach $N_R = 4$	Upper Bound Approach $N_R = 4$
4-QAM $N_T = 2$	2	6	1.5	2
4-QAM $N_T = 4$	4	10	1.8	4
16-QAM $N_T = 4$	6	14	3.5	9

3.5 Chapter Summary

The performance analysis for conventional QSM system employing both the lower bound approach and the upper bound approach to quantify the average BER performance for M-QAM QSM system with optimal detector over an i.i.d entries with zero mean and unit variance $CN(0,1)$, Rayleigh fading channel $\boldsymbol{H}$ was formulated. The analytical result is relatively tight with the simulated BER of the QSM system as shown in Figure 3-2, 3-3 and 3-4, respectively, thereby validating the analytical framework.

CHAPTER 4

Adaptive Quadrature Spatial Modulation

4 Introduction

Over the years, MIMO systems have shown significant promise with respect to its potential for high capacity coupled with superior system reliability. This has led to a vast amount of interest in the research community. However, challenges to its realization exist.

SM [15], is an example of a MIMO scheme that utilizes transmit antennas in an innovative manner to make MIMO systems more realizable. SM uses the spatial dimension to convey additional information via a single RF chain. The requirement for a single RF chain in SM eliminates IAS and ICI, which are the major limitations experienced in MIMO systems. However, practical realization is challenging due to high CC.

Similarly, SM still has a major criticism of its data rate enhancement, which is found to be proportional to logarithm base-two of the total number of transmit antennas. This is unlike other spatial multiplexing techniques, such as V-BLAST [11], where the data rate increases linearly, with the number of transmit antennas. This led to the proposal of an enhanced spectral efficiency SM-based scheme termed QSM [33].

QSM, extends its spatial constellation to the in-phase and quadrature-phase dimensions to enhance the overall spectral efficiency of the system. In QSM, the constellation symbols are further decomposed into their real and imaginary components, while the in-phase dimension transmits the real part of the decomposed symbol and the imaginary part of the symbol is transmitted via the quadrature-phase dimension of the spatial dimension. The decomposed symbols are modulated into the cosine and sine carriers, respectively, thereby eliminating ICI completely. QSM exhibits significant enhancement in terms of BER when compared to SM of the same spectral efficiency [16, 33].

Meanwhile, it has been proven that, it is impossible to construct full-rate, full-diversity schemes with spatial multiplexing such as V-BLAST, which can give high multiplexing gain with linear complexity [24, 39]. Likewise, it has been investigated in [25] and [26], that link adaptation can further improve the error performance of a MIMO scheme, such that, with a very good link, a highly efficient modulation scheme is employed and vice versa [27].

Several innovative MIMO systems have been investigated to further improve the reliability and reduce CC of the system. For example, in [24], MA-GSM is investigated to reduce the hardware complexity of the novel GSM system. The proposed MA-GSM uses multiple transmit antennas to convey information similar to the conventional SM system. Significant improvement was achieved in terms of hardware complexity in the proposed system.

The extremely high CC in [25] was reduced in [26], employing different modulation order candidates with the same target spectral efficiency coupled with transmit-mode switching. Furthermore, a decision metric of the transmission mode with the minimum BER as the transmission candidate mode at that transmission instant was employed to further improve the error performance of the system. In [25, 26], the candidate mode that maximizes the minimum Euclidean distance is selected as the transmission mode.

Another link adaptation technique was proposed in [30], which employs pre-processing, pre-coder formulation techniques at the transmitter prior to transmission, in order to achieve transmit diversity, maximizing the minimum Euclidean distance among the pre-coded codewords.

A similar approach to [30], was investigated in [31], using two different transmit pre-coding algorithms. One is based on maximizing the minimum Euclidean distance between the constellation points at the receiver as against among the codewords in [30]. The second algorithm in [31] is based on minimizing the BER, which can jointly maximize the overall Euclidean distance between the received signal points. The Monte Carlo simulation results demonstrate that the second algorithm proposed in [31] (employing the minimum BER) achieved significant improvement when compared to the first algorithm (maximizing the minimum Euclidean distance).

Similar to [26], a system which employs both modulation order and transmit-mode switching to further improve the error performance of the QSM system is proposed. A decision metric of the minimum IBEP is used to select the candidate transmission mode at every transmission instant in order to further decrease the CC imposed by the decision metric in [26] and [31]. Capitalizing on the LUT computation technique, which can be adopted to the system to further reduce the CC imposed on the system.

In addition, employing ML detection at the receiver, to search across $N_T^2 M$ constellation points and to estimate the transmitted symbol together with the antenna index at each transmission instant. This increases the CC at the receiver [40, 41]. According to [42], incorporating EDAS can further improve the error performance of the system but this impose a high CC.

However, a LCTAS proposed in [19, 23], exhibits a low CC compared to the EDAS technique. This can further reduce the CC at the receiver by evaluating the channel amplitude and antenna correlation at each transmission instant. Employing LCTAS, the CC of the system is reduced than employing EDAS approach, but EDAS exhibits a superior error performance.

In this chapter, we propose the combination of both the LCTAS coupled with a link adaptation technique and the minimum IBEP is employed as the decision metric. We aim at further improving the reliability of the QSM scheme.

4.1 System Model for the Proposed Adaptive Quadrature Spatial Modulation

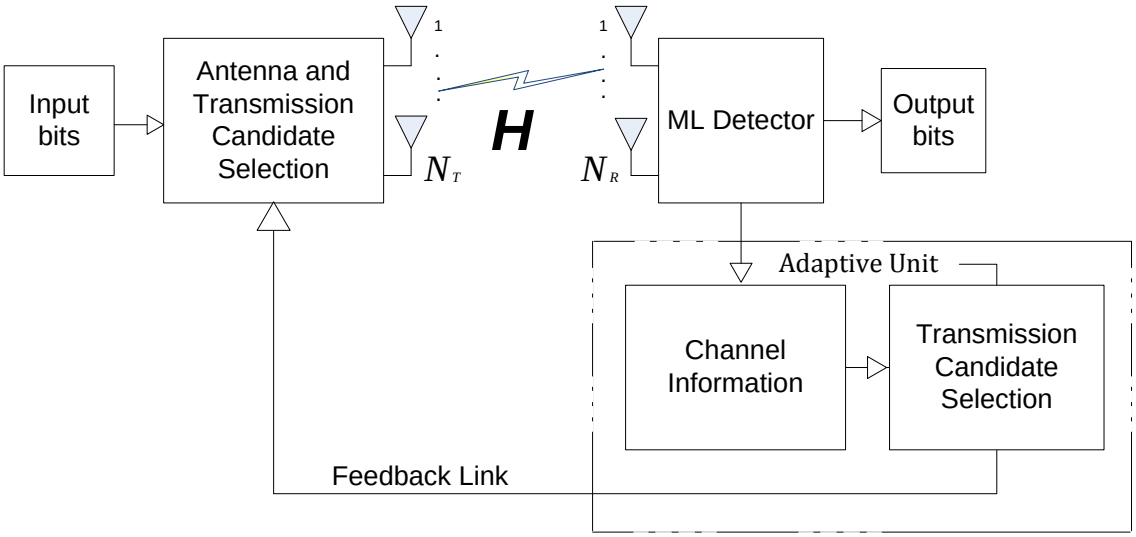

Figure 4-1 System model of the proposed AQSM

Figure 4-1 describes the system model of the proposed AQSM scheme, equipped with N_T transmit antennas and N_R receive antennas coupled with a low-bandwidth feedback link, interconnecting the adaptive unit to the transmitter, which selects the transmission candidate mode at each transmission instant.

The proposed AQSM employs μ unique candidate transmission modes, to satisfy a target spectral efficiency $m = \log_2(MN_T^2)$. For example, we consider 16-QAM with $N_T = 2$, which gives a spectral efficiency of 6 b/s/Hz. Likewise, 4-QAM with $N_T = 4$ with a spectral efficiency of 6 b/s/Hz. Each candidate mode employs the QSM scheme with different modulation orders such that the target spectral efficiency is met.

The IBEP of each candidate transmission mode is computed and the optimum candidate (candidate mode with the minimum IBEP) is selected as the transmission mode for the subsequent transmission interval. More specifically, when the channel is slowly varying, the adaptive unit computes the IBEP for each candidate transmission mode to select the candidate mode with the minimum IBEP and sends this information to the transmitter through a feedback link. The transmitter then employs the corresponding transmission candidate mode for the next channel use.

The $\log_2 M$ bits modulate the M-QAM symbols and $2\log_2 N_T$ bits are used to select the active transmit antenna to transmit the decomposed symbol, respectively. The lower bound approach used to evaluate the IBEP is formulated in the next sub-section.

4.2 Analysis of Instantaneous Bit Error Probability for Adaptive Quadrature Spatial Modulation

The IBEP of each candidate transmission mode is computed at every transmission instant, similar to [43] and [44]. In formulating the IBEP for the proposed AQSM system, the IBEP of the antenna detection and symbol detection are computed independently as follows:

1. Compute the symbol error considering a single transmit antenna is employed for transmission. However, if two transmit antennas are employed for transmission, the IBEP for the symbol detection is computed similar to [44].
2. Formulate the IBEP associated to employing single antenna for transmission for either of:
    a) If one antenna is employed for transmission and detected as one antenna, i.e. the antenna index is correctly detected at the receiver.
    b) If one antenna is employed and detected as two antennas
3. Formulate the IBEP associated to employing two antennas for transmission for either of:
    c) Two antennas are employed for transmission and detected as two antennas, i.e. the antenna index is correctly detected.
    d) Two antennas are employed and detected as a single antenna.

The transmission candidate mode, which minimizes the IBEP is activated in the subsequent signalling interval. The IBEP for the k^{th}, $k \in [1: N_T^2]$, transmit antenna setting may be defined using a lower-bound approach as [7]:

$$P_e^i(k) \geq 1 - ((1 - P_a^i(k))(1 - P_b^i(k))) = P_a^i(k) + P_b^i(k) - P_a^i(k)P_b^i(k) \quad (4\text{-}1)$$

where $P_a^i(k)$ is the IBEP of antenna detection and $P_b^i(k)$ is the IBEP of symbol detection.

In addition, we may partition the range $k \in [1: N_T^2]$ into $\ell \in [1: N_T]$, when a single antenna is used for transmission, i.e. the transmit antenna index that modulates the real and imaginary parts of the constellation symbol are the same and $r \in [1: N_T(N_T - 1)]$ when two transmit antennas are employed, i.e. the transmit antenna index that modulates the real and imaginary parts of the constellation symbol are different. Considering that the constellation symbol is further decomposed into real and imaginary parts and two transmit antennas are employed to transmit the decomposed symbol, respectively.

4.2.1 Analysis of Symbol Estimation Employing a Single Transmit Antenna

Considering the symbol error detection of the proposed AQSM when the active transmit antennas that transmit the real and imaginary parts are the same, i.e. $\ell \in [1: N_T]$. Considering square M-QAM [36]:

$$P_b^i(\ell) = \frac{1}{\log_2 M}\left(4A_\ell^M(\rho) - \left(4A_\ell^M(\rho)\right)^2\right) \quad (4\text{-}2)$$

where $A_\ell^M(\rho) = \left(1 - \frac{1}{\sqrt{M}}\right) Q\left(\sqrt{\frac{3\|\boldsymbol{h}_\ell\|_F^2 \rho}{M-1}}\right)$, $\ell \in [1: N_T]$.

4.2.2 Analysis of Symbol Estimation Employing Two Transmit Antennas

When the active transmit antennas are different, i.e. there are $r \in [1: N_T(N_T - 1)]$ possibilities. In this condition, the in-phase and quadrature-phase components of the transmitted symbol are considered independently, i.e. each antenna is transmitting L-PAM $(L^2 = M)$, as they are symmetrical. Therefore, the overall IBEP can be derived in a similar manner to [7] and [44].

$$P_b^i(r) = P_{bR}^i(r) + P_{bI}^i(r) - P_{bR}^i(r)P_{bI}^i(r) \quad (4\text{-}3)$$

where $P_{bR}^{i}(r)$ is the probability of error when the in-phase part of the symbol is transmitted and $P_{bI}^{i}(r)$ is the probability of error when the quadrature-phase part of the symbol is transmitted.

In [44], P_{bR}^{i} and P_{bI}^{i} are computed as:

$$P_{bR}^{i}(r) = \left[\frac{2(L-1)}{L\log_2 L} Q\left(\sqrt{\frac{6\rho_1}{2(L^2-1)}}\right)\right] \tag{4-4}$$

$$P_{bI}^{i}(r) = \left[\frac{2(L-1)}{L\log_2 L} Q\left(\sqrt{\frac{6\rho_2}{2(L^2-1)}}\right)\right] \tag{4-5}$$

where $\rho_1 = \rho\left\|\boldsymbol{h}_{\ell R}^{k}\right\|_F^2$, $\boldsymbol{h}_{\ell R}^{r}$ is the channel selected by the transmit antenna selection in transmitting the in-phase component of the received signal and $\rho_2 = \rho\|\boldsymbol{h}_{\ell I}^{r}\|_F^2$, where $\boldsymbol{h}_{\ell I}^{r}$ is the channel selected by the transmit antenna selection in transmitting the quadrature-phase component of the symbol.

P_{bR}^{i} and P_{bI}^{i} can be evaluated by employing an alternative form of the Q-function in (4-4) and (4-5), respectively, and using the MGF [36], the LUT approach is employed for the CC of the Q-function.

4.2.3 Analysis of Transmit Antenna Index Estimation Employing a Single Transmit Antenna

The IBEP for antenna detection, P_a^i can be computed similar to [7], for which two cases exist. For example, when single antenna is employed and when two antennas are employed.

Case 1: At first, only one transmit antenna is considered, i.e. there are $\ell \in [1: N_T]$ possibilities, but this can be detected as any of N_T^2 possibilities.

a) Considering the antenna used for transmission to be detected as a single antenna $\hat{\ell}$ for $\ell \neq \hat{\ell}$:

$$P_a^i(\ell_1) \leq \sum_j N(\ell, \hat{\ell})\, \mathrm{P}\left(\boldsymbol{x}_{jq} \to \boldsymbol{x}_{\hat{j}q}\right) \to \sum_{q=1}^{M}\sum_{\hat{l}=1}^{Nt} \frac{N(\ell, \hat{\ell})\, \mathrm{P}\left(\boldsymbol{x}_{jq} \to \boldsymbol{x}_{\hat{j}q}\right)}{M\log_2(N_T^2)}$$

$$P_a^i(\ell_1) \leq \sum_j N(l,\hat{l}) \Pr(\boldsymbol{x}_{jq} \to \boldsymbol{x}_{\hat{j}q}) \to \sum_{q=1}^{M} \sum_{\hat{l}=1}^{Nt} \frac{N(l,\hat{l}) \Pr(x_{jq} \to x_{\hat{j}q})}{M \log_2(N_T^2)} \quad (4\text{-}6)$$

where $\mathrm{P}(\boldsymbol{x}_{jq} \to \boldsymbol{x}_{\hat{j}q})$ is the PEP of choosing $\boldsymbol{x}_{\hat{j}q}$ and given that $\boldsymbol{x}_{jq}$ was transmitted and $N(\ell, \hat{\ell})$ is the associated number of bit errors between transmit antenna pairs.

The PEP can be derived as shown in [45] as:

$$\begin{aligned} P(\boldsymbol{x}_{\ell q} \to \boldsymbol{x}_{\hat{\ell} q} | \boldsymbol{H}) &= P\left(\left\| \boldsymbol{y} - \sqrt{\rho} \boldsymbol{h}_{\hat{\ell}} x_q \right\|_F < \left\| \boldsymbol{y} - \sqrt{\rho} \boldsymbol{h}_{\ell} x_q \right\|_F \right) \\ &= P\left(\left\| \sqrt{\rho} \boldsymbol{h}_{\ell} x_q - \sqrt{\rho} \boldsymbol{h}_{\hat{\ell}} x_q + \boldsymbol{\eta} \right\|_F < \| \boldsymbol{\eta} \|_F \right) \end{aligned} \quad (4\text{-}7)$$

Using the triangle inequality [7], i.e. $|x| - |y| \leq |x + y| \leq |x| + |y|$ across a combined SNR and simplifying, (4-7) becomes:

$$P(\boldsymbol{x}_{\ell q} \to \boldsymbol{x}_{\hat{\ell} q} | \boldsymbol{H}) = Q\left(\frac{\left\| \sqrt{\rho} \boldsymbol{h}_{\ell} x_q - \sqrt{\rho} \boldsymbol{h}_{\hat{\ell}} x_q \right\|_F}{2\sqrt{N_R}} \right) \quad (4\text{-}8)$$

In estimating the transmit antenna index at the receiver, the antenna used for transmission can be detected as a single antenna or as two antennas, out of all the N_T^2 possibilities. The analysis for estimating the transmit antenna index when single transmit antenna is used and detected as two antennas is as follows:

b) Considering the antenna used for transmission to be detected as two antennas $\hat{r}$ for $r \neq \hat{r}$:

$$P_a^i(\ell_2) \leq \sum_{q=1}^{M} \sum_{r=1}^{N_T(N_T-1)} \frac{N(\ell, r) \, \mathrm{P}(\boldsymbol{x}_{\ell q} \to \boldsymbol{x}_{rq} | \boldsymbol{H})}{M \log_2(N_T^2)} \quad (4\text{-}9)$$

The PEP can be computed as:

$$P(\boldsymbol{x}_{\ell q} \to \boldsymbol{x}_{rq}|\boldsymbol{H}) = P\left(\left\|\boldsymbol{y} - \sqrt{\rho/2}\boldsymbol{h}_r^1 x_{Re}^q - i\sqrt{\rho/2}\boldsymbol{h}_r^2 x_{Im}^q\right\|_F < \left\|\boldsymbol{y} - \sqrt{\rho}\boldsymbol{h}_\ell x_q\right\|_F\right)$$

$$= Q\left(\frac{\left\|\sqrt{\rho}\boldsymbol{h}_\ell \boldsymbol{x}_q - \sqrt{\rho/2}\boldsymbol{h}_r^1 x_{Re}^q - i\sqrt{\rho/2}\boldsymbol{h}_r^2 x_{Im}^q\right\|_F}{2\sqrt{N_R}}\right) \quad (4\text{-}10)$$

Thus, the upper bound is defined as:

$$P_a^i(k) \le P_a^i(\ell_1) + P_a^i(\ell_2) \quad (4\text{-}11)$$

4.2.4 Analysis of Transmit Antenna Index Estimation Employing Two Transmit Antennas

Considering another case, where two transmit antennas are employed for transmission, this can be detected as any of the N_T^2 possibilities. This can be analysed as follows:

Case 2: Two transmit antennas were employed, i.e. there are $r \in [1: N_T(N_T - 1)]$ possibilities, but this can be detected as any one of N_T^2 possibilities.

i) Considering it to be detected as a single antenna ℓ:

$$P_a^i(r_1) \le \sum_{q=1}^{M}\sum_{\ell=1}^{N_T} \frac{N(r,\ell)P(\boldsymbol{x}_{rq} \to \boldsymbol{x}_{\ell q}|\boldsymbol{H})}{M\log_2 N_T^2} \quad (4\text{-}12)$$

Thus, the PEP becomes:

$$P(\boldsymbol{x}_{rq} \to \boldsymbol{x}_{\ell q}|\boldsymbol{H}) = P\left(\left\|\boldsymbol{y} - \sqrt{\rho}\boldsymbol{h}_\ell x_q\right\|_F < \left\|\boldsymbol{y} - \sqrt{\rho/2}\boldsymbol{h}_r^1 x_{Re}^q - i\sqrt{\rho/2}\boldsymbol{h}_r^2 x_{Im}^q\right\|_F\right)$$

$$= Q\left(\frac{\left\|\sqrt{\rho/2}\boldsymbol{h}_r^1 x_{Re}^q + j\sqrt{\rho/2}\boldsymbol{h}_r^2 x_{Im}^q - \sqrt{\rho}\boldsymbol{h}_\ell x_q\right\|_F}{2\sqrt{N_R}}\right) \quad (4\text{-}13)$$

ii) Considering it to be detected as two antennas $\hat{r}$ for $r \neq \hat{r}$:

$$P_a^i(r_2) \le \sum_{q=1}^{M}\sum_{\hat{r}=1}^{N_T(N_T-1)} \frac{N(r,\hat{r})P(\boldsymbol{x}_{rq} \to \boldsymbol{x}_{\hat{r}q}|\boldsymbol{H})}{M\log_2(N_T^2)}$$

$$P_a^i(r_2) \leq \sum_{q=1}^{M} \sum_{\hat{r}=1}^{N_T(N_T-1)} \frac{N(r,\hat{r}) P(x_{rq} \to x_{\hat{r}q} | \boldsymbol{H})}{M \log_2(N_T^2)} \tag{4-14}$$

The PEP is given as:

$$P(\boldsymbol{x}_{rq} \to \boldsymbol{x}_{\hat{r}q} | \boldsymbol{H}) = P\left(\left\| \boldsymbol{y} - \sqrt{\rho/2} \boldsymbol{h}_{\hat{r}}^1 x_{Re}^q - j\sqrt{\rho/2} \boldsymbol{h}_{\hat{r}}^2 x_{Im}^q \right\|_F < \left\| \boldsymbol{y} - \sqrt{\rho/2} \boldsymbol{h}_r^1 x_{Re}^q - j\sqrt{\rho/2} \boldsymbol{h}_r^2 x_{Im}^q \right\|_F \right)$$

$$= Q\left(\frac{\left\| \sqrt{\rho/2} \boldsymbol{h}_r^1 x_{Re}^q + j\sqrt{\rho/2} \boldsymbol{h}_r^2 x_{Im}^q - \sqrt{\rho/2} \boldsymbol{h}_{\hat{r}}^1 x_{Re}^q - j\sqrt{\rho/2} \boldsymbol{h}_{\hat{r}}^2 x_{Im}^q \right\|_F}{2\sqrt{N_R}} \right) \tag{4-15}$$

Thus, the upper bound is defined as:

$$P_a^i(k) \leq P_a^i(r_1) + P_a^i(r_2) \tag{4-16}$$

4.3 The Proposed AQSM System Based on Euclidean Distance Antenna Selection

4.3.1 Background

In [21], an optimal transmit antenna selection was investigated in SM, based on maximizing the minimum Euclidean distance to further improve the average error performance of the system.

Considering the PEP given in [21]:

$$P_e \cong \lambda \cdot Q\left(\sqrt{\frac{1}{2} \min_{x_{q_1} \neq x_{q_2} \in \boldsymbol{\chi}} \left\| \boldsymbol{H}'(x_{q_1} - x_{q_2}) \right\|_F^2} \right) = \lambda \cdot Q\left(\sqrt{\frac{1}{2} d_{min}^2(\boldsymbol{H}')} \right) \tag{4-17}$$

where λ is the number of neighbor points and $d_{min}^2(\boldsymbol{H}') = \min_{x_{q_1} \neq x_{q_2} \in \boldsymbol{\chi}} \left\| \boldsymbol{H}'(x_{q_1} - x_{q_2}) \right\|_F^2$ is the squared minimum Euclidean distance between the pair of neighbor symbols.

In maximizing the minimum Euclidean distance, the selected antennas can be chosen using:

$$\ell_{selected} = \underset{\ell \in 1:N_s}{\operatorname{argmin}} \left\{ \min_{x_{q_1} \neq x_{q_2} \in \boldsymbol{\chi}} \left\| \boldsymbol{H}_\ell (x_{q_1} - x_{q_2}) \right\|_F^2 \right\}$$

$$\ell_{selected} = \text{argmin}_{\ell \in 1:N_s} \left\{ \min_{\boldsymbol{x}_{q_1} \neq \boldsymbol{x}_{q_2} \in \boldsymbol{\chi}} \left\| \boldsymbol{H}_{\ell} (\boldsymbol{x}_{q_1} - \boldsymbol{x}_{q_2}) \right\|_F^2 \right\} \tag{4-18}$$

It can be verified that the minimum distance between any pair of symbols for M-QAM is two [21]. Therefore, for $i = j$, which is the diagonal element, $D_{i,i}$ becomes:

$$D_{i,i} = \min_{x_{q_1} \neq x_{q_2} \in \boldsymbol{\chi}} \left\| \boldsymbol{h}_j \right\|_F^2 \left| x_{q_1} - x_{q_2} \right|^2, q \in [1:M] \tag{4-19}$$

However, for $i \neq j$, (4-19) can be modified such that (4-19) becomes:

$$\begin{bmatrix} \boldsymbol{h}_{iI} & -\boldsymbol{h}_{iQ} & \boldsymbol{h}_{jI} & -\boldsymbol{h}_{jQ} \\ \boldsymbol{h}_{iQ} & \boldsymbol{h}_{iI} & \boldsymbol{h}_{jQ} & \boldsymbol{h}_{jI} \end{bmatrix} \begin{bmatrix} x_{q_{1I}} \\ x_{q_{1Q}} \\ -x_{q_{2I}} \\ -x_{q_{2Q}} \end{bmatrix} \tag{4-20}$$

Employing the QR decomposition of the channel matrix for factorization into an orthogonal matrix $\boldsymbol{Q}$ and upper triangular matrix $\boldsymbol{R}$ we arrive at:

$$D_{i,j} = \min_{\boldsymbol{x}_{q_1} \neq \boldsymbol{x}_{q_2} \in \boldsymbol{\chi}} \left\| \boldsymbol{R} x_q \right\|_F^2 \tag{4-21}$$

since $\boldsymbol{Q}^H \boldsymbol{Q} = I_{|\boldsymbol{Q}|}$.

where x_q is the constellation symbol.

Then, $\boldsymbol{R} x_q$ can be defined as:

$$\boldsymbol{R} x_q = \begin{bmatrix} r_{1,1} & 0 & r_{1,3} & r_{1,4} \\ 0 & r_{2,2} & r_{2,3} & r_{2,4} \\ 0 & 0 & r_{3,3} & 0 \\ 0 & 0 & 0 & r_{4,4} \end{bmatrix} \begin{bmatrix} x_{q_{1I}} \\ x_{q_{1Q}} \\ -x_{q_{2I}} \\ -x_{q_{2Q}} \end{bmatrix} \tag{4-22}$$

where $x_{q_{1I}}$ and $x_{q_{1Q}}$ are the decomposed x_q symbol into in-phase and quadrature-phase parts, respectively.

Evaluating and hard limiting $\left\|\boldsymbol{R}x_q\right\|_F^2$ to determine x_1, such that:

$$r_{1,1}x_{1I} - r_{1,3}x_{2I} - r_{1,4}x_{2Q} = 0,$$
$$r_{2,2}x_{1Q} - r_{2,3}x_{2I} - r_{2,4}x_{2Q} = 0 \quad (4\text{-}23)$$

Then, define the parameter u,

$$u = r_{i,3}x_{2I} + r_{i,4}x_{2Q}/r_{i,i},\ i = 1,2. \quad (4\text{-}24)$$

where $u = u_1 + ju_2$

The algorithm of the proposed AQSM system based on EDAS proceeds in Algorithm 1:

4.3.2 Algorithm 1

Step 1: Construct an $N_R \times N_{Total}$ channel matrix, where $N_{Total} > N_T$.

Step 2: Compute all the possible combination of the antenna subset N_s using $\binom{N_{Total}}{N_T}$.

Step3: Construct the upper triangular matrix **D** of dimension $N_{Total} \times N_{Total}$.

Step 4: Populate the non-zero elements following the procedure in [21]:

$$\mathrm{D_{i,i}} = \min_{x_{q_1} \neq x_{q_2} \in \boldsymbol{\chi}} \left\|\boldsymbol{h}_j\right\|_F^2 \left|x_{q_1} - x_{q_2}\right|^2 \quad (4\text{-}25)$$

For M-QAM the minimum distance between any pair of symbols can be verified to be two. Therefore, $d_{min} = 2$.

$$\mathrm{D_{i,j}} = \min_{\substack{x_{1I},x_{2I}\in N_1 \\ x_{1Q},\,x_{2Q}\in N_2}} \left\| \begin{bmatrix} r_{1,1}x_{1I} - r_{1,3}x_{2I} - r_{1,4}x_{2Q} \\ r_{2,2}x_{1Q} - r_{2,3}x_{2I} - r_{2,4}x_{2Q} \\ -r_{3,3}x_{2I} \\ -r_{4,4}x_{2Q} \end{bmatrix} \right\|_F^2 \tag{4-26}$$

where N_1 and N_2 represent the separated $\sqrt{M}$ −PAM sets for the in-phase and quadrature-phase components, respectively.

Step 5: Solve for ℓ_{selected} using:

$$\ell_{\text{selected}} = \underset{\ell\in 1:N_s}{\operatorname{argmin}} \left\{\min\left(\mathbf{D}(\ell)\right)\right\} \tag{4-27}$$

The selected (ℓ_{selected}) set is then used as the chosen transmit antenna subset for single-active transmission.

Step 6: Compute the overall IBEP for each transmission candidate mode.

Employing (4-2) to compute the symbol error P_b^i, if single transmit antenna was employed for transmission. However, if two transmit antennas are employed for transmission (4-4) and (4-5) are used to compute the symbol error P_b^i.

Step 7: Compute the antenna index error P_a^i for each transmission candidate mode. Such that, if single transmit antenna is employed for transmission and detected as a single transmit antenna or two transmit antennas, the probability of error is computed using (4-6) and (4-9). The result is substituted into (4-11) to evaluate the antenna error P_a^i.

Similarly, if two transmit antennas are employed for transmission and detected as a single transmit antenna or two transmit antennas, the probability of error is computed using (4-12) and (4-14). The result is substituted into (4-16) to evaluate the antenna error P_a^i. The overall IBEP P_e^i can now be computed for each transmission candidate mode substituting the resulting P_a^i and P_b^i into (4-1).

Step 8: Choose the transmission candidate mode with the minimum IBEP as the transmission candidate at that transmission instant.

Consider an example of candidate transmission Mode 1 = 4 × 4, 4-QAM and candidate transmission Mode 2 = 2 × 4, 16-QAM, with $N_{Total} = 6$, each with a target spectral efficiency

of $m = 6$ bits, with a total of two (2) transmission candidate modes, i.e. $\mu = 2$. An algorithm based on this example proceeds as follows:

Example 1

Step 1: Construct an 4×6 channel matrix, where $N_{Total} = 6$.

Step 2: Compute all the possible combination of the antenna subset N_s using $\binom{6}{4}$.

Step3: Construct the upper triangular matrix **D** of dimension $N_{Total} \times N_{Total}$ i.e. 6×6.

Step 4: Solve for ℓ_{selected} using:

$$\ell_{\text{selected}} = \underset{\ell \in 1:N_s}{\text{argmin}}\{\min(\mathbf{D}(\ell))\} \tag{4-28}$$

The selected (ℓ_{selected}) set is then used as the chosen transmit antenna subset for single-active transmission.

Step 5: Compute the overall IBEP for each transmission candidate mode.

Compute the symbol error P_b^i using (4-2), if single transmit antenna was employed for transmission. However, if two transmit antennas are employed for transmission (4-4) and (4-5) are used to compute the symbol error P_b^i.

Step 6: The antenna index error P_a^i is computed for each transmission candidate mode. Such that, if single transmit antenna is employed for transmission, the probability of error is computed using (4-6) and (4-9). Then, the result is substituted into (4-11) to evaluate the antenna error P_a^i.

Likewise, if two transmit antennas are employed for transmission, the probability of error is computed using (4-12) and (4-14). The result is substituted into (4-16) to evaluate the antenna error P_a^i. The overall IBEP P_e^i can now be computed for each transmission candidate mode substituting the resulting P_a^i and P_b^i into (4-1). Such that for the first transmission candidate mode $k = 16,\ k \in [1: N_T^2]$. Likewise, for the second transmission candidate mode $k = 4,\ k \in [1: N_T^2]$.

Step 7: Choose the transmission candidate mode with the minimum IBEP as the transmission candidate at that transmission instant.

It was observed from the Monte Carlo simulation results obtained, that EDAS further improves the error performance of the conventional QSM system but the CC imposed on the system is high. This is due to the exhaustive search of the system between transmit vector to select the best transmit antenna to yield the best error performance result. However, in [19], the proposed LCTAS investigated for SM, demonstrates a low CC when compared to EDAS proposed in [22]. Therefore, comparing the optimal transmit antenna selection (EDAS) employed earlier in AQSM scheme with LCTAS in AQSM system in terms of CC and error performance, will be worthwhile. This motivates for investigating LCTAS in the system.

4.4 The Proposed AQSM System with Antenna Selection Based on Channel Amplitude and Antenna Correlation

In the proposed topology, an important part to consider is the LCTAS aimed at further reducing the CC employing a similar approach to [19]. Employing the concept of channel amplitude with a decision of the larger the amplitude of the channel the better it is, as investigated in [20] and antenna correlation, which concept was investigated in [46], discarding transmit antennas based on high correlation. Employing both channel amplitude and antenna correlation, which are sub-optimal techniques will impose a very low CC [19]. This motivates the application of this technique to the proposed AQSM. The algorithm for the LCTAS and computing the IBEP is presented in Algorithm 2:

4.4.1 Algorithm 2

Step 1: Construct an $N_R \times N_{T_1}$ dimension channel matrix, where N_{T_1} is the number of transmit antennas of the transmission candidate mode with the highest number of N_T.

$$\boldsymbol{H} = [\boldsymbol{h}_1\ \boldsymbol{h}_2\ \boldsymbol{h}_3 \ldots\ \boldsymbol{h}_{N_T}] \tag{4-29}$$

Step 2: Compute the channel amplitude using $\|\boldsymbol{H}\|_F$ for the above channel constructed in *Step 1* and sort in descending order.

Step 3: Choose $N_T + 1$ such that the dimension matrix becomes $N_R \times (N_T + 1)$, i.e.

$$\boldsymbol{H} = [\boldsymbol{h}_1\ \boldsymbol{h}_2 \ldots\ \boldsymbol{h}_{N_T+1}] \tag{4-30}$$

Step 4: Calculate the angle of correlation of the channel combination similar to [17] and [47] using:

$$\theta = \arccos\left(\frac{|\boldsymbol{h}_a{}^H \boldsymbol{h}_b|}{\|\boldsymbol{h}_a\|_F \|\boldsymbol{h}_b\|_F}\right) \tag{4-31}$$

where $\boldsymbol{h}_a$ and $\boldsymbol{h}_b$ are the possible antenna pairs in the corresponding vectors in the channel matrix $\boldsymbol{H}$

Step 5: Arrange the angle of correlation in vectors and eliminate the smallest angle (highest correlation) from the channel $N_T + 1$ computed in Step 4.

Step 6: Compute the overall IBEP for each transmission candidate mode using (4-1).

Considering the symbol error P_b^i for each transmission candidate mode with two cases, i.e. when the active antenna is the same and when they are different such that:

if $(\ell_R = \ell_I)$

(4-2) is evaluated

else

The probability of when the real part of the symbol is transmitted and when the imaginary part of the symbol is transmitted are computed. Considering L-PAM being symmetrical, (4-4) and (4-5) are evaluated and substituted to (4-3) to give P_b^i

Step 7: Compute the antenna index error P_a^i for each transmission candidate mode with four possible cases i.e. when single antenna is employed and is detected as single antenna, when single antenna is employed and detected as two antennas, when two antennas is employed and is detected as one and when two antenna are used and detected as two antennas. All these cases are used to compute the antenna index error P_a^i such that:

if $(\ell_R = \ell_I)$

Compute the probability of when single antenna is employed and detected as single antenna $P_a^i(\ell_1)$ or detected as two antennas $P_a^i(\ell_2)$. Using (4-6) and (4-9) to evaluate $P_a^i(\ell_1)$ and $P_a^i(\ell_2)$ respectively. Substitute the result into (4-11) to evaluate the antenna error P_a^i

else

The probability of when two antennas are employed and detected as single antenna $P_a^i(r_1)$ or detected as two antennas $P_a^i(r_2)$. Using (4-12) and (4-14) to evaluate $P_a^i(r_1)$ and $P_a^i(r_2)$ respectively and substituting the result in (4-16) to evaluate P_a^i. Therefore, the overall IBEP P_e^i can now be computed for each transmission mode substituting the resulting P_a^i and P_b^i into (4-1).

Thus, the mode with the minimum IBEP is selected for transmission at that particular transmission instant.

Consider an example of candidate transmission Mode 1 = 4 × 4, 4-QAM and candidate transmission Mode 2 = 2 × 4, 16-QAM, each with a target spectral efficiency of $m = 6$ bits, with a total of two (2) transmission candidate modes, i.e. $\mu = 2$. An algorithm based on this example proceeds as follows:

Example 2

Step 1: Construct a 4 × 4 dimension channel matrix:

$$\boldsymbol{H} = [\boldsymbol{h}_1\ \boldsymbol{h}_2\ \boldsymbol{h}_3\ \boldsymbol{h}_4] \tag{4-32}$$

Step 2: Compute the channel amplitude using $\|\boldsymbol{H}\|_F$ for the constructed channel in *Step 1*.

Step 3: Arrange the resulting channel amplitude in descending order and choose the first desired $N_T + 1$, which is to be used for transmission in the second candidate transmission mode setting, i.e in this case $N_T = 2$ eliminating the channel with the highest channel amplitude. Assuming we are left with:

$$\boldsymbol{H} = [\boldsymbol{h}_2\ \boldsymbol{h}_3\ \boldsymbol{h}_1] \tag{4-33}$$

Step 4: Calculate the angle of correlation for $\binom{3}{2}$ = 3 pairs for the channel combination similar to [17] and [47] using:

$$\theta = \arccos\left(\frac{|\boldsymbol{h}_a{}^H \boldsymbol{h}_b|}{\|\boldsymbol{h}_a\|_F \|\boldsymbol{h}_b\|_F}\right) \tag{4-34}$$

Step 5: Arrange the angle of correlation into vectors and eliminate the smallest angle (highest correlation) from the channel $N_T + 1$ computed in *Step 3* above. This leaves us with the desired $N_R \times N_T$, i.e. 2×4 channel matrix needed for transmission for the second transmission candidate mode setting. Assuming channel $\boldsymbol{h}_2$ is eliminated.

$$\boldsymbol{H} = [\boldsymbol{h}_3\ \boldsymbol{h}_1] \tag{4-35}$$

Step 6: Compute the symbol error P_b^i for each transmission candidate mode with two cases, i.e. when the active antenna is the same and when they are different such that:

if $(\ell_R = \ell_I)$

(4-2) is evaluated to compute P_b^i for each transmission candidate mode

else

Evaluate (4-4) and (4-5) for each transmission candidate mode and substitute it to (4-3) to give P_b^i considering L-PAM been symmetrical.

Step 7: Compute the antenna index error P_a^i for each transmission candidate mode such that:

if $(\ell_R = \ell_I)$

Compute the probability of when single antenna is employed and is been detected as single antenna $P_a^i(\ell_1)$ or detected as two antennas $P_a^i(\ell_2)$. Using (4-6) and (4-9) to evaluate $P_a^i(\ell_1)$ and $P_a^i(\ell_2)$ respectively and substitute it in (4-11) to compute the antenna error P_a^i

else

Compute the probability of when two antennas are employed and are been detected as single antenna $P_a^i(r_1)$ or detected as two antennas $P_a^i(r_2)$. Using (4-12) and (4-14) to evaluate $P_a^i(r_1)$ and $P_a^i(r_2)$ respectively and substituting in (4-16) to evaluate P_a^i. Therefore, the overall IBEP P_e^i can be computed for each transmission mode substituting the resulting P_a^i and P_b^i into (4-1). Such that for the first transmission candidate mode $k = 16,\ k \in [1: N_T^2]$. Hence, the IBEP is computed as:

$$P_e^i = \frac{1}{16}\left(P_e^i(1) + \ P_e^i(2) + \cdots + P_e^i(16)\right) \tag{4-36}$$

Similarly, for the second transmission candidate mode $k = 4,\ k \in [1: N_T^2]$. Thus, the IBEP is computed as:

$$P_e^i = \frac{1}{4}\left(\ P_e^i(1) + \ P_e^i(2) + \cdots + P_e^i(4)\right) \tag{4-37}$$

4.5 Computational Complexity Analysis for the Proposed Topology

In this section, the CC for EDAS and the LCTAS coupled with the proposed decision metric is computed. The CC is analysed, employing the floating points of operation (flops) approach similar to [23] and [48].

4.5.1 Computational Complexity Analysis for Transmit Antenna Selection based on EDAS

The CC of the proposed antenna selection coupled with the decision metric is computed and compared to each other. In [22], the CC of EDAS antenna selection was computed and presented as:

$$\partial_{EDAS-SM} = N_{Total}(2N_R - 1) + 64\binom{N_{Total}}{2}\left(N_R - \frac{2}{3}\right)\frac{M}{N} \tag{4-38}$$

where N is the number of points in the quadrant [22].

4.5.2 Computational Complexity Analysis for Transmit Antenna Selection based on Channel Amplitude and Antenna Correlation

The CC imposed on the LCTAS based on amplitude and correlation (LCTAS-A-C) was evaluated in [19]. In *Step 2*, $2N_R$ flops is required resulting in a total complexity of $(2N_R - 1)N_{Total}$. *Step 4*, involves all possible combinations of antenna pairs for channel gain sub-matrices, resulting in $(6N_R + 2)\binom{N_L}{2}$ flops. Hence, the overall CC imposed in the system is:

$$\partial_{LCTAS-AC} = N_{Total}(2N_R - 1) + 2(6N_R + 2)\binom{N_L}{2} \tag{4-39}$$

where N_L is the total number of the selected channels.

Employing (4-38) and (4-39) the numerical comparison in terms of complexity between both systems is computed in Table 4-1

Table 4-1 Numerical Comparison of Computational Complexity of EDAS and LCTAS-A-C

	EDAS		LCTAS-A-C	
Configuration	$M = 4$	$M = 16$	$N_L = 3$	$N_L = 5$
$N_R = 2$	2,577.36	10,255.44	102	298
$N_R = 4$	6,442	25,639.44	198	562

In comparing the CC of EDAS with LCTAS-A-C, tabulated in Table 4-1. It was observed that EDAS impose a higher CC on the system and LCTAS-A-C reduce the CC by approximately 96%.

4.5.3 Computational Complexity Analysis for the Proposed Topology Based on EDAS

In this section, the CC is analysed employing flops approach similar to [48]. Algorithm 3 will be used to analyse the CC of the decision metric of the minimum IBEP considering a single mode transmission. In [19], the CC of the QR decomposition for EDAS was evaluated using flops which impose $64\binom{\frac{1}{2}N_{Total}}{2}\left(N_R - \frac{2}{3}\right)\frac{M}{N}$. $\|\boldsymbol{H}\|_F$ requires N_R flops for single mode transmission in Step 6 and LUT approach can be employed for $Q(\cdot)$, resulting in a total of 6 flops in (4-2) and 8 flops in (4-4), which is evaluated N_T^2 times. Similarly, Step 7 impose

$4N_R + 1$ flops and required across $M(N_T - 1)$ which is evaluated N_T times. Hence, the overall CC becomes:

$$\partial_{AQSM-EDAS} = \sum_{l=1}^{\mu} 14\, N_T^{2^l} + M^l N_T^l \left(N_T^j - 1\right) + 5N_R + 65 \binom{\frac{1}{2} N_{Total}}{2} \left(N_R - \tfrac{2}{3}\right) \tfrac{M}{N} \quad (4\text{-}40)$$

where M^l and N_T^l is the modulation order and the transmit antenna pairs of the l^{th} transmission candidate mode and μ is the number of candidate transmission modes.

4.5.4 Computational Complexity Analysis for the Proposed Topology Based on Channel Amplitude and Antenna Correlation

The example given in the previous section will be used to analyse the CC of the decision metric of the minimum IBEP considering a single mode transmission. In Step 2, considering a single transmission $\|\boldsymbol{H}\|_F$ requires N_R flops. Likewise, the inner product of the numerator of Step 4 requires $N_T(2N_R - 1) + 2N_R - 1$ flops and the denominator requires $\binom{N_T + 1}{2} 2N_R$ flops. Similarly, the CC of Step 6 is computed as follows:

Considering $\|\boldsymbol{h}_l\|_F$ has been computed earlier and the LUT approach can be employed for $Q(\cdot)$, this leaves us with a total of 6 flops in (4-2) and 8 flops in (4-4), considering a single mode which is evaluated N_T^2 times. Likewise, Step 7 impose $4N_R + 1$ flops and required across $M(N_T - 1)$ and evaluated N_T times. Thus, the overall CC becomes:

$$\partial_{AQSM} = \sum_{j=1}^{\mu} 14\, N_T^{2^j} + M^j N_T^j \left(N_T^j - 1\right) + 7N_R + N_T(2N_R - 1) + 2N_R \binom{N_T + 1}{2} \quad (4\text{-}41)$$

where M^j and N_T^j is the modulation order and the transmit antenna pairs of the j^{th} transmission candidate mode and μ is the number of candidate transmission modes.

Employing (4-40) and (4-41) the numerical comparison in terms of complexity between both systems is computed in Table 4-2:

Table 4-2 Numerical Comparison of Computational Complexity of AQSM-EDAS and AQSM-LCTAS

Configuration	AQSM-EDAS $M = 4$	AQSM-LCTAS $M = 4$	AQSM-EDAS $M = 16$	AQSM-LCTAS $M = 16$
$N_T = 2$ $N_R = 2$	270,333	98	292,333	122
$N_T = 2$ $N_R = 4$	282,333	132	304,333	156
$N_T = 4$ $N_R = 2$	478,333	334	620,333	478
$N_T = 4$ $N_R = 4$	490,333	396	632,333	540

It was observed that AQSM-EDAS impose a higher CC on the system when compared to AQSM-LCTAS. Approximately 64% reduction was achieved in AQSM-LCTAS system.

4.6 Numerical Analysis of the BER Performance for Adaptive Quadrature Spatial Modulation

The Monte Carlo simulation results of the proposed AQSM is presented in this section. The performance comparison between the conventional QSM and AQSM system of the same spectral efficiency of 6 b/s/Hz and 8 b/s/Hz, both with two receive antennas ($N_R = 2$) is shown in Figure 4-2 and Figure 4-3, respectively.

In Figure 4-2, the proposed AQSM system exhibits a significant improvement with a gain of 4 dB at a BER of 10^{-5} over a conventional QSM system of the same spectral efficiency of 6 bits with two candidate transmission modes of 4×2 4-QAM and 2×2 16-QAM.

Likewise, in Figure 4-3, AQSM shows significant enhancement with a gain of 2 dB at a BER of 10^{-5} over similar conventional QSM system with the same spectral efficiency of 8 bits, also with two candidate transmission mode of 4×2 16-QAM and 2×2 64-QAM.

The EDAS was implemented with the proposed AQSM comparing the error performance with the LCTAS; the Monte Carlo simulation result shows that the error performance for AQSM-EDAS is better than AQSM-LCTAS with a gain of 2 dB at a BER of 10^{-5} as seen in Figure 4-3. Although, the performance was improved but the CC of AQSM-EDAS is higher than that of AQSM-LCTAS. As summarized in Table 4-1 and Table 4-2, respectively.

AQSM achieves a better performance than a conventional QSM system. Also, as the spectral efficiency increases, the overall performance of the system begins to improve at a very high SNR as shown in Figure 4-3.

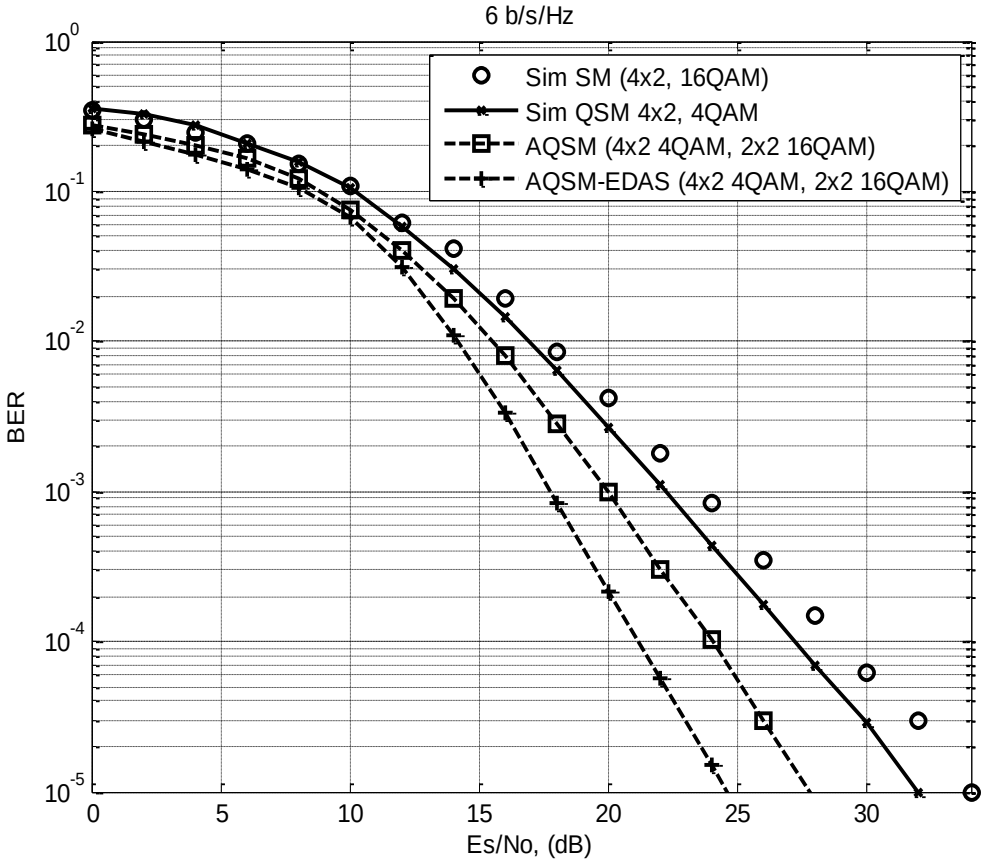

Figure 4-2 Comparison of BER performance between AQSM, AQSM-EDAS and QSM for 6 b/s/Hz considering $N_R = 2$.

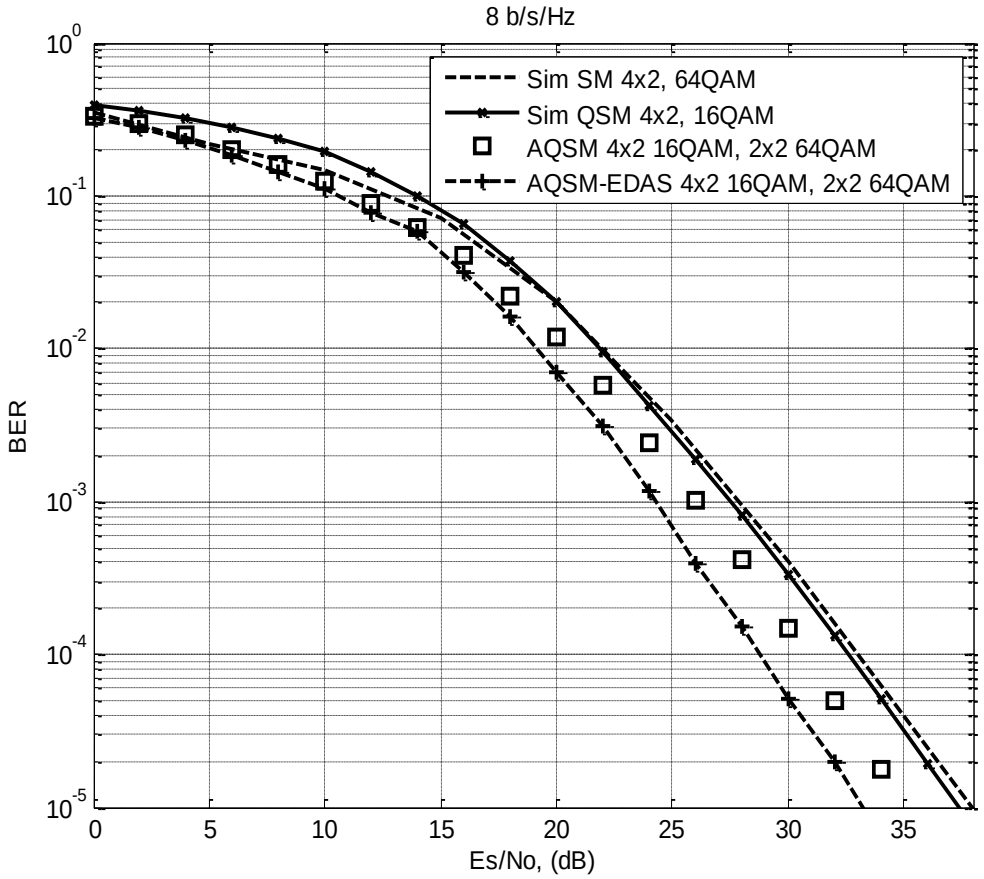

Figure 4-3 Comparison of BER performance between AQSM, AQSM-EDAS and QSM for 8 b/s/Hz considering $N_R = 2$.

Table 4-3 SNR gain (dB) achieved, with respect to the proposed AQSM

Scheme	SNR gain of AQSM-EDAS at a BER of 10^{-5}	
	6 b/s/Hz	8 b/s/Hz
SM	9 dB	4 dB
QSM	7 dB	3 dB
AQSM-LCTAS	2 dB	2 dB

The SNR gain achieved by AQSM with respect to SM, QSM and AQSM-EDAS schemes are tabulated in Table 4-3. It was observed that AQSM-EDAS achieved a gain of 9 dB and 4 dB over SM of spectral efficiency 6 b/s/Hz and 8 b/s/Hz, respectively. Likewise, 7 dB and 3 dB

gain was achieved, respectively, over QSM. However, AQSM-EDAS achieved a gain of 2 dB in the 6 b/s/Hz and 8 b/s/Hz system, respectively over AQSM-LCTAS.

4.7 Chapter Summary

An adaptive scheme for M-QAM QSM system was proposed and analysed. The AQSM system introduced link adaptation to conventional QSM scheme, by employing the minimum IBEP as the decision metric coupled with EDAS and LCTAS. As a result, both transmit and receive diversity were achieved. A closed-form of IBEP for AQSM in Rayleigh flat-fading channel was derived and the Monte Carlo simulation results demonstrate the accuracy of the result obtained.

The proposed AQSM outperform the conventional QSM system of the same spectral efficiency in terms of BER. A gain of approximately 4 dB was achieved as shown in Figure 4-2.

The Monte Carlo simulation results show that the error performance of AQSM-EDAS is better than AQSM-LCTAS with a gain of 2 dB at a BER of 10^{-5} in 6 b/s/Hz and 8 b/s/Hz system, as shown in Figure 4-2 and Figure 4-3, respectively. Although, the performance was improved but the CC of AQSM-EDAS is higher than that of AQSM-LCTAS.

The CC analysis of the proposed system shows a reduced CC in the decision metric as compared with [31].

The two schemes differ in terms of detection and performance analysis. These are summarized by the following points:

1. Detection: Both the AQSM and QSM systems utilize ML detection, which perform an optimal joint detection of transmit antenna index and symbol vector. Meanwhile, the AQSM system is equipped with LCTAS to eliminate the worse channel at every transmission instant. This in-turn reduces the complexity in the joint detection at the receiver.
2. Performance analysis: In both schemes, a lower bound approach is used to obtain the theoretical analytic result. In QSM system, the lower bound approach is used to evaluate the bit error probability of the antenna index and bit error probability of the symbol, while in AQSM system, the lower bound approach is employed to further evaluate the IBEP, which is used as the decision metric.

CHAPTER 5

Conclusion and Future Work

5 Conclusion

In this dissertation, link adaptation technique was investigated in QSM to further improve the error performance of the system, employing a low CC decision metric, in the form of the IBEP.

MIMO systems and its transmission model was introduced in Chapter 1, stating the advantages and the limitations experienced in the scheme. In Chapter 2, a single stream MIMO technique SM, which improves the major limitations of IAS and ICI experienced in conventional MIMO schemes with the performance analysis of the system was presented in Chapter 2.

The average BER of M-QAM QSM in a Rayleigh fading channel was derived in Chapter 3 employing a lower bound approach. The analytical result of the proposed lower bound approach validates the Monte Carlo simulation results more closely from low to high SNRs region when compared to the asymptotic union bound for $N_R = 2$ and $N_R = 4$.

In Chapter 4, the proposed AQSM scheme aimed at improving the error performance of the conventional QSM system. The main idea behind the scheme was to employ different transmission candidate modes configuration settings to achieve a target spectral efficiency. The IBEP for each candidate mode was computed prior to transmission and the candidate mode with the minimum IBEP was selected as the transmission mode.

In addition, EDAS, an optimal based TAS between the transmit vector to select the best transmit antenna was incorporated with the proposed AQSM system. A notable disadvantage with optimal antenna selection is the high CC they impose on the system. However, a LCTAS was employed to further reduce the CC imposed on the system. It was observed that the error performance of the AQSM system with EDAS was superior to the proposed AQSM system with LCTAS. Although, the performance was better, but the CC imposed on the system is higher.

It was evident from the Monte Carlo simulation results that the proposed AQSM system achieved a significant enhancement over the conventional QSM system. In Table 5-1, the SNR gain achieved using AQSM-EDAS at a BER of 10^{-5} over AQSM-LCTAS, SM and QSM scheme is summarized.

Table 5-1 SNR gain (dB) of AQSM as compared to QSM and SM at a BER of 10^{-5}

Scheme	SNR gain of AQSM-EDAS at a BER of 10^{-5}	
	6 b/s/Hz	8 b/s/Hz
SM	9 dB	4 dB
QSM	7 dB	3 dB
AQSM-LCTAS	2 dB	2 dB

Furthermore, in Chapter 4 of this dissertation, the difference between AQSM-EDAS, an optimal technique and AQSM-LCTAS, a sub-optimal technique in terms of CC was evaluated.

Table 5-2 Numerical comparison of Computational Complexity of AQSM-EDAS and AQSM-LCTAS

Configuration	AQSM-EDAS $M = 4$	AQSM-LCTAS $M = 4$	AQSM-EDAS $M = 16$	AQSM-LCTAS $M = 16$
$N_T = 2$ $N_R = 2$	270,333	98	292,333	122
$N_T = 2$ $N_R = 4$	282,333	132	304,333	156
$N_T = 4$ $N_R = 2$	478,333	334	620,333	478
$N_T = 4$ $N_R = 4$	490,333	396	632,333	540

The evaluation of the CC of AQSM-LCTAS and AQSM-EDAS revealed that AQSM-LCTAS exhibit lower CC than AQSM-EDAS by approximately 64%. The difference between AQSM-EDAS and AQSM-LCTAS in terms of CC is tabulated in Table 5-2.

5.1 Future Work

Future work can be aimed at providing research advances in the following direction:

1. Improving reliability: introducing pre-coder designs and channel coding to the conventional QSM scheme and the proposed AQSM system can further improve the reliability of the system. Researching into this technique to further enhance the BER of the system will be useful.

2. Decreasing CC: ML was employed in the QSM system and in the proposed AQSM system. The imposed CC on the system can be further reduced by incorporating low-complexity detection technique. One idea is to apply a sub-optimal detector to the system.

REFERENCE

[1] A. Goldsmith, Wireless Communications, 1st ed., New York: Cambridge University Press, 2005.

[2] S. S. E. Krouk, Modulation and Coding Techniques in Wireless Communications: John Wiley & Sons Ltd, 2011.

[3] M. K. Simon, Digital Communication over Fading Channels: Wiley-Interscience Publication, 2010.

[4] Wikipedia, " MIMO " available at https://en.wikipedia. org/w/index.php? title= MIMO &oldid=723879399, Jun. 2016.

[5] H. Junkai and Y. Liang, "MIMO MRT-MRC Systems with Rate Adaptive Modulation," in *Proceedings of the Networks Security, Wireless Communications and Trusted Computing, (NSWCTC 2009)*, pp. 12-16, Apr. 2009.

[6] X. Wang, J. Geng, X. Zhang, and D. Yang, "Spatial Multiplexing with Opportunistic Multiuser Scheduling in Ad Hoc Networks," in *Proceedings of the IEEE Vehicular Technology Conference (VTC Fall)*, pp. 1-5, Sep. 2012.

[7] N. R. Naidoo, H. Xu, T. Quazi, "Spatial modulation: optimal detector asymptotic performance and multiple-stage detection," *IET Communications,* vol. 5, no. 10, pp. 1368 - 1376, Jul. 2010.

[8] N. R. Naidoo, "Performance analysis and enhancement schemes for spatial modulation," Msc Thesis, School of Electrical, Electronics and Computer Engineering, University of KwaZulu-Natal, Dec. 2010.

[9] Cisco, "Multhipath and Diversity," available at http://www.cisco.com/c/ en/us/support /docs/wireless-mobility/wireless-lan-wlan/27147-multipath.html, Jun. 2016.

[10] T. Ngoc-Anh, V. V. Mai, T. C. Thang, and A. T. Pham, "Impact of reflections and ISI on the throughput of TCP over VLC networks with ARQ-SR protocol," in *Proceedings of the IEEE 4th International Conference on Photonics (ICP)*, pp. 172-174, Oct. 2013.

[11] P. W. Wolniansky, G. J. Foschini, G. D. Golden, and R. Valenzuela, "V-BLAST: an architecture for realizing very high data rates over the rich-scattering wireless channel," in *Proceedings of the International Symposium on Signals, System and Electronics. (ISSSE 98)*, pp. 295-300, Sep. 1998.

[12] H. Hass. R. Y. Mesleh, L. Yeonwoo and Y. Sangboh, "Interchannel Interferenece Avoidance in MIMO Transmission by Exploiting Spatial Information," in *Proceedings of the IEEE 16th International Symposium on Personal, Indoor and Mobile Radio Communications, (PIMRC 2005)*, pp. 141-145, Sep. 2005.

[13] L. Tsung-Hsien, "Analysis of the Alamouti STBC MIMO System With Spatial Division Multiplexing Over the Rayleigh Fading Channel," *IEEE Transactions on Wireless Communications*, vol. 14, no. 9, pp. 5156-5170, May. 2015.

[14] E. Basar, U. Aygolu, E. Panayirci, and H. V. Poor, "Space-Time Block Coded Spatial Modulation," *IEEE Transactions on Wireless Communications,* vol. 59, no. 3, pp. 823-832, Mar. 2011.

[15] R. Y. Mesleh, H. Haas, S. Sinanovic, A. Chang Wook, and Y. Sangboh, "Spatial Modulation," *IEEE Transactions on Vehicular Technology*, vol. 57, no. 4, pp. 2228-2241, Jul. 2008.

[16] J. Jeganathan, A. Ghrayeb, and L. Szczecinski, "Spatial modulation: optimal detection and performance analysis," *IEEE Wireless Communications Letters*, vol. 12, no. 8, pp. 545-547, Aug. 2008.

[17] Z. Jianping, "Signal Vector Based List Detection for Spatial Modulation," *IEEE Wireless Communications Letters*, vol. 1, no. 4, pp. 265-267, May. 2012.

[18] W. Jintao, J. Shuyun, and S. Jian, "Generalised Spatial Modulation System with Multiple Active Transmit Antennas and Low Complexity Detection Scheme," *IEEE Transactions on Wireless Communications*, vol. 11, no. 4, pp. 1605-1615, Apr. 2012.

[19] N. Pillay and H. Xu, "Low-complexity transmit antenna selection schemes for spatial modulation," *IET Communications*, vol. 9, no. 2, pp. 239-248, Jan. 2015.

[20] R. Rajashekar, K. V. S. Hari, and L. Hanzo, "Antenna Selection in Spatial Modulation Systems," *IEEE Wireless Communications Letters*, vol. 17, no. 3, pp. 521-524, Jan. 2013.

[21] N. Pillay and H. Xu, "Comments on "Antenna Selection in Spatial Modulation Systems", *IEEE Wireless Communications Letters*, vol. 17, no. 9, pp. 1681-1683, Aug. 2013.

[22] W. Nan, L. Wenlong, M. Hongzhi, J. Minglu, and H. Xu, "Further Complexity Reduction Using Rotational Symmetry for EDAS in Spatial Modulation," *IEEE Communications Letters*, vol. 18, no. 10 pp. 1835-1838, Oct. 2014.

[23] N. Pillay, H. Xu, "Low Complexity Detection and Transmit Antenna Selection for Spatial Modulation," *SAIEE Africa Research Journal*,Vol. 105, no. 1, Mar. 2014.

[24] F. Jinlin, H. Chunping, X. Wei, Y. Lei, and H. Yonghong, "Generalised spatial modulation with multiple active transmit antennas," in *Proceedings of the IEEE GLOBECOM Workshops (GC Wkshps)*, pp. 839-844, Dec. 2010.

[25] Y. Ping, X. Yue, Y. Yi, and L. Shaoqian, "Adaptive Spatial Modulation for Wireless MIMO Transmission Systems," *IEEE Communications Letters*, vol. 15, no. 6, pp. 602-604, Jun. 2011.

[26] Y. Ping, X. Yue, L. Lei, T. Qian, Y. Yi, and L. Shaoqian, "Link Adaptation for Spatial Modulation With Limited Feedback," *IEEE Transactions on Vehicular Technology*, vol. 61, no. 8, pp. 3808-3813, Oct. 2012.

[27] T. ABC, "Link Adaptation," available at http://www.telecomabc.com/l/link-adaptation .html, Dec. 2015.

[28] P. Yang, Y. Xiao, S. Li, and L. Hanzo, "A Low-Complexity Power Allocation Algorithm for Multiple-Input Multiple-Output Spatial Modulation Systems," *IEEE Transactions on Vehicular Technology*, vol. 65,no. 3, pp. 1819-1825, Mar. 2015.

[29] M. Di Renzo and H. Haas, "Improving the performance of space shift keying (SSK) modulation via opportunistic power allocation," *IEEE Communications Letters*, vol. 14, no. 6, pp. 500-502, Jun. 2010.

[30] L. Ming-Chun, C. Wei-Ho, and L. Ta-Sung, "Generalized Precoder Design Formulation and Iterative Algorithm for Spatial Modulation in MIMO Systems With CSIT," *IEEE Transactions on Wireless Communications*, vol. 63, no. 4, pp. 1230-1244, Apr. 2015.

[31] P. Yang, Y. L. Guan, Y. Xiao, M. Di Renzo, S. Li, and L. Hanzo, "Transmit Pre-coded Spatial Modulation: Maximizing the Minimum Euclidean Distance Versus Minimizing the Bit Error Ratio," *IEEE Transactions on Wireless Communications*, vol. 15,no. 3, pp. 2054-2068, Nov. 2015.

[32] S. Mei-Yin and C. J. Kuo, "Real-time compression artifact reduction via robust nonlinear filtering," in *Proceedings of the International Conference on Image Processing (ICIP 99)*, vol.2, pp. 565-569, Oct. 1999.

[33] R. Mesleh, S. S. Ikki, and H. M. Aggoune, "Quadrature Spatial Modulation," *IEEE Transactions on Vehicular Technology*, vol. 64, no. 6, pp. 2738-2742, Jul. 2014.

[34] R. Mesleh and S. S. Ikki, "A High Spectral Efficiency Spatial Modulation Technique," in *Proceedings of the 80th IEEE Vehicular Technology Conference (VTC Fall 2014)*, pp. 14-17, Sep. 2014.

[35] R. Rajashekar, K. V. S. Hari, and L. Hanzo, "Quantifying the Transmit Diversity Order of Euclidean Distance Based Antenna Selection in Spatial Modulation," *IEEE Signal Processing Letters*, vol. 22, no. 9, pp. 1434-1437, Mar. 2015.

[36] H. Xu, "Symbol error probability for generalized selection combining reception of M-QAM " *SAIEE Africa Research Journal*, vol. 100, no. 3, pp 68 - 71, Sep. 2009.

[37] S. Naidu, N. Pillay, H. Xu, "A Study of Quadrature Spatial Modulation," in *Proceedings of the Southern Africa Telecommunication Networks and Applications Conference (SATNAC)*, Sep. 2015.

[38] B. M. Mthethwa and H. Xu, "Adaptive M-ary quadrature amplitude spatial modulation," in *IET Communications*, vol. 6, no. 18, pp. 3098-3108, Dec. 2012.

[39] E. Basar and U. Aygolu, "Full-rate full-diversity STBCs for three and four transmit antennas," *Electronics Letters*, vol. 44, no. 18, pp. 1076-1077, Aug. 2008.

[40] H. Xu, "Simplified maximum likelihood-based detection schemes for M-ary quadrature amplitude modulation spatial modulation," *IET Communications*, vol. 6, no. 11, pp. 1356-1363, Jul. 2012.

[41] M. Hongzhi and J. Minglu, "A Low-Complexity ML Detection Algorithm for Spatial Modulation Systems With M- PSK Constellation," *IEEE Communications Letters*, vol. 18, no. 8, pp. 1375-1378, Aug 2014.

[42] R. Rajashekar, K. V. S. Hari, K. Giridhar, and L. Hanzo, "Performance Analysis of Antenna Selection Algorithms in Spatial Modulation Systems with Imperfect CSIR," in *Proceedings of the 19th European Wireless Conference (EW)*, pp. 16-18, Apr. 2013.

[43] S. A. Chandra, C. Bose, "M-QAM Error Performance with Equal Gain Diversity over Rayleigh Fading Channel," in *Proceedings of the Embedded Systems, Mobile Communications and Computing*, pp 21-26, Aug. 2007.

[44] A. K. Sah and A. K. Chaturvedi, "An upper bound on the performance of K-best detection for MIMO systems," in *Proceedings of the International Conference on Signal Processing and Communications (SPCOM)*, pp. 22-25, Jul. 2014.

[45] N. Pillay, H. Xu, "Adpative Generalized Spatial Modulation," *IET Wireless Communications Letters*, (under review).

[46] Z. Zhou, N. Ge, and X. Lin, "Reduced-Complexity Antenna Selection Schemes in Spatial Modulation," *IEEE Communications Letters,* vol. 18, no. 1, pp. 14-17, Jan. 2014.

[47] N. Pillay and H. Xu, "Comments on "Signal Vector Based Detection Scheme for Spatial Modulation", *IEEE Communications Letters,* vol. 17, no. 1, pp. 2-3, Jan. 2013.

[48] A. M. Elshokry, "Complexity and performance evaluation of detection schemes for spatial multiplexing in MIMO systems" Msc Thesis, Department of Electrical Engineering, Islamic University Gaza, Aug. 2010.